APW CALCULATION OF THE ELECTRON-PHONON INTERACTION IN SOLID ARGON AND NEON

By

JOSEPH PATRICK WORTH

A DISSERTATION PRESENTED TO THE GRADUATE COUNCIL
OF THE UNIVERSITY OF FLORIDA
IN PARTIAL FULFILLMENT OF THE REQUIREMENTS FOR THE
DEGREE OF DOCTOR OF PHILOSOPHY

UNIVERSITY OF FLORIDA

1976

This dissertation is dedicated to the memory of Professor John C. Slater, whose contributions to modern physics had a profound influence on present day theories of solid state physics and quantum chemistry. It seems only fitting that this work, which makes use both of Professor Slater's Xα model and APW method, should be dedicated to the memory of his role in the development of the theory of condensed matter. That Professor Slater could not be made aware of the results of this work is regrettable.

ACKNOWLEDGEMENTS

Dr. Samuel B. Trickey, my dissertation advisor, is gratefully acknowledged as the source for the ideas in this dissertation and for his help, advice, and encouragement (in all forms!) throughout the course of this work. His dedication, enthusiasm, and sense of humor have helped me in my efforts to understand and complete this work. I particularly want to thank him for the tremendous opportunity to accompany him on his year's sabbatical leave at the I.B.M. Research Lab in San Jose, California. Without that year of uninterrupted study, concentrated work, and computational freedom, this dissertation would not have been possible. I thank Dr. John Connolly for bringing the Golibersuch article to my attention. I am also grateful to the many members of the Quantum Theory Project for their help.

The International Business Machines Corporation's Research Laboratory at San Jose, California is to be thanked for allowing a year's visit during Dr. Trickey's sabbatical. Drs. T.R. Koehler, P. Bagus, D. Haarer, and G. Castro and many other people of the Research Lab are to be thanked for their hospitality and help during my visit.

This dissertation was made possible through the financial support of the National Science Foundation, the computing support of the Northeast Regional Data Center of the State University System of Florida, and the computing and laboratory facilities of the I.B.M. Research Laboratory in San Jose, California.

PREFACE

"The whole thing is a low put-up job on our noble credulity," said Sam.

NORMAN LINDSAY, The Magic Pudding

And, so, if you can't dazzle 'em with brilliance, ...

TABLE OF CONTENTS

PAGE

ACKNOWLEDGEMENTS iii

PREFACE iv

ABSTRACT vii

CHAPTER

I. INTRODUCTION 1

1-1. Purpose of Calculation 1

1-2. Assumptions and Approximations 2

1-3. Outline of Calculation 4

II. FORMAL THEORY AND METHODS OF CALCULATION 7

2-1. Born-Oppenheimer Theory for Crytalline Solids 7

2-2. The Xα Hamiltonian 11

2-3. The APW Method 13

2-4. The Fröhlich Hamiltonian 16

2-5. The Derivation of the Form for the EPME 27

III. RESULTS OF CALCULATIONS 34

3-1. APW Energy Band Calculation of Argon and Neon ... 34

3-2. The SCH Phonon Spectra of Argon and Neon 38

3-3. The Perturbed Phonon Spectra of Argon and Neon .. 41

IV. CONCLUSIONS 43

APPENDICES

I. SELF-CONSISTENT HARMONIC THEORY AND LENNARD-JONES PAIR POTENTIALS 46

II. GROUP THEORETICAL EXPLANATION OF THE TRANSITION SELECTION RULES 51

III. EXPLICIT DERIVATION AND FORMULAE FOR THE EPME 72

IV. DESCRIPTION OF COMPUTER PROGRAMS AND CODES 77

LIST OF REFERENCES 80

BIOGRAPHICAL SKETCH 83

Abstract of Dissertation Presented to the Graduate Council
of the University of Florida in Partial Fulfillment of the Requirements
for the Degree of Doctor of Philosophy

APW CALCULATION OF THE ELECTRON-PHONON INTERACTION IN SOLID ARGON AND NEON

By

Joseph Patrick Worth

December, 1976

Chairman: Samuel B. Trickey
Major Department: Physics

The electron-phonon interaction in solid argon and neon was calculated within the self-consistent field augmented plane wave local exchange (SCF APW-Xα) model. The Fröhlich Hamiltonian, which uses the electron-phonon interaction in the form of a transition probability matrix element, was assumed to be appropriate for describing corrections to the phonon spectra. Second order perturbation theory involving the calculated electron-phonon matrix element (EPME) was used to compute corrections to phonons unperturbed by the electron-phonon interaction. The unperturbed phonons were calculated within the self-consistent harmonic (SCH) approximation, assuming a superposition of Lennard-Jones pair potentials. The pair potential parameters were not determined empirically, but were fitted to the calculated equilibrium lattice constant or the experimental lattice constant and to the corresponding calculated APW-Xα cohesive energies. Explicit expressions for the EPME were derived in the APW formalism, as were selection rules between representations

involved in the relevant inter-band transitions. To calculate the EPME numerically, computer codes were written and tested. The perturbed phonons, calculated as a test of the EPME, were found to be in poor agreement for neon and in good agreement for argon, a distinction which can be traced directly to the shortcomings in the original Xα calculation on neon, and not to the method in general.

CHAPTER I

INTRODUCTION

1-1. Purpose of Calculation

It is essential to study the interaction of electrons with the lattice vibrations or phonons in a crystal if the basic properties and characteristics of solids are to be understood. Such effects as superconductivity in metals, phonon dispersion anomalies, and electronic specific heat enhancement may be calculated once one has detailed knowledge of the electron-phonon (EP) interaction.

However, the aim in this work is not so ambitious as a calculation of the above effects. Rather, the present effort is to develop a formal computational procedure to calculate from first principles the EP interaction in a physically realistic model of an insulator. Once the method has been justified and demonstrated to be feasible, the application to the effects caused by the EP interaction may be done.

A seemingly practical and sound method of calculating the EP interaction was advanced almost 10 years ago by Golibersuch.[1] His idea for calculating the electron-phonon matrix element (EPME) was to exploit certain features of Slater's augmented plane wave (APW)[2] method for the calculation of the energy bands in a solid.

In his article, Golibersuch justified a certain specific form of the EPME, then explicitly derived the computational formulae in terms of some of the quantities available in conventional APW computer codes.[3] However, no calculations based on his method have ever appeared in the literature. The reason for this absence of calculations is probably the complicated nature of his formulae; in particular, the occurrence of double sums over angular momenta (two ℓ sums and two m sums) which include some rather intricate spherical harmonic transformation matrices.

An examination of Golibersuch's paper shows that his method does not take explicit advantage of the muffin-tin symmetry inherent in the usual APW method.[2] Also he does not consider an insulator, although his justification of the EPME is general. Therefore, a method that exploits the muffin-tin symmetry has been developed for filled valence band solids (not necessarily insulators), and is the subject of the present work. It should be emphasized however, that the EPME used in this work is based on the form justified by Golibersuch.

To test the calculation of the EPME, the effect of the electron interaction on the phonon spectra of solid argon and neon has been computed. Though this test is rather severe (as will be explained subsequently), it demonstrates both the power and the limitations inherent in our procedure.

1-2. Assumptions and Approximations

Perhaps the most crucial assumption for the overall calculation is that of allowing the nuclei and electrons to interact among themselves and each other only through short-ranged screened potentials. Such screened potentials are inherent in the self-consistent field (SCF) APW description of the electrons and the Fröhlich Hamiltonian[4] which will be used to calculate energy corrections to the phonons arising from the EP interaction. A truly basic approach would be to calculate first the bare nuclear interaction and then screen this interaction with an electron distribution whose response is described by a dielectric function. An approach along these lines has been derived by Sinha[5] for the APW method, but does not appear to be computationally feasible. Although the formal theory of microscopic lattice dynamics has been developed by Toya,[6] Pick,[7] and others[8] through the dielectric response concept, few, if any, practical numerical calculations have been attempted. This work, even with its approximations, represents an attempt at a calculation based in principle on microscopic lattice dynamics.

The Born-Oppenheimer adiabatic theory and approximation[9] are assumed to be applicable in calculating the electronic wave functions for a static lattice. The formal equivalence between the Fröhlich theory and the adiabatic theory has been pointed out previously,[10] but will be derived explicitly in Chapter II in the present context.

In order to carry out an APW calculation of the now-traditional muffin-tin type (the sort originally discussed by Slater[2]), a one-electron potential must be available. Even at the level of Hartree-Fock theory, the generation of such a potential for a crystal is an almost prohibitively difficult task. A great deal of effort has gone into developing methods which circumvent this difficulty at the cost of the introduction of certain _ad hoc_ physical assumptions. The most widely studied of these schemes approximates exchange and correlation contributions to the potential along the lines of exchange (designated as X) in the electron gas[11] with the added flexibility of one parameter (designated as α); the model is therefore known as the "$X\alpha$" model.[12]

In this study of lattice dynamics, the APW muffin-tin potential associated with a particular nucleus is assumed to move rigidly with that nucleus. This "rigid ion" approximation[13] allows the total solid potential to be a superposition of all muffin-tin potentials centered on the nuclear locations.

For the nuclear motion, the potentials are assumed to be harmonic; i.e. the effect of the force is linear in the displacement. Even the self-consistent harmonic (SCH)[14] approximation used to calculate the unperturbed phonons has as its basis functions harmonic solutions, though the method itself contains implicit and inherent multi-phonon processes (to infinite order).[14] The total static lattice potential is assumed to be describable in terms of the cohesive energy and lattice constant of the solid. This description is parameterized through a set of Lennard-Jones pair potential constants.[15] The fitted constants are used in a Lennard-Jones pair potential which is superposed to yield the total lattice potential.

All these assumptions and approximations will be reviewed and examined in the proper context in Chapter II where the formal theory is developed. In light of the conclusions reached in Chapter IV, the severity or appropriateness of the approximations and assumptions will be discussed.

1-3. Outline of Calculation

The first phase of the calculation consists in obtaining the static electronic Bloch wave functions at a given lattice constant in the APW basis. The number of eigenvalues and Bloch wave functions are determined by the type and number of atoms in the solid. Self-consistency is obtained through one of three criteria: convergence (or more exactly, iteration to iteration stability) on the pressure, one-electron eigenvalues (i.e. band energies), or potential. Usually when one of these criteria is achieved, the others are also fairly well satisfied.

When the Bloch functions, energy eigenvalues, and self-consistent potential are obtained to desired accuracy, the cohesive energy of the solid is calculated at the assumed lattice constant. The cohesive energy and the assumed lattice constant then can be used to parameterize the electronic contribution to the bulk, static solid in terms of Lennard-Jones pair potential parameters.[15] This parameterization describes the static solid by a lattice sum involving all distinguishable pairs in the solid. The 12-6 form of the potential[15] is used for computational convenience in obtaining the phonon spectrum of the solid.

Next, the SCH formalism is applied to the given total lattice potential, based on the Lennard-Jones potential superposition. A phonon spectrum is calculated to a specified level of precision by iterative solution of the SCH dynamical matrix eigenvalue problem (see Appendix I). This set of phonons constitutes the unperturbed phonons (i.e. phonons unperturbed by explicit interaction with the electrons).

In principle, the EPME should be calculated for all transitions between occupied bands and empty bands. Since, however, the transition probability is dominated by a factor inversely proportional to the energy difference between the states of the transition, the main contributing transitions are taken to be between the highest single valence band states and the lowest single conduction band states. In the rare gas insulators (e.g. argon and neon), this means only transitions from the highest p-like valence band states to the lowest s-like conduction band states. The fact that these bands exhibit simple symmetry properties throughout the zone is a great convenience for computation.

The EPME is calculated throughout the entire first Brillouin zone (BZ) (see Appendix II). The square of the EPME is used to find a second order perturbation energy correction to the phonons. The contributions to the energy shifts for a phonon of a given vector and polarization are governed by certain selection rules that relate this phonon to the electronic irreducible representations (which label the electron wave vector and state). These allowed electronic corrections are then summed over the entire first BZ.

This is a basic description of the procedure involved in the EPME and phonon correction calculation. Chapter II gives a theoretical and formal justification for the procedures outlined here. Chapter III includes the results, commentary, and comparison with known quantities. Conclusions regarding the results, their implications for the assumptions, and the method in general are presented in Chapter IV. There are four Appendices in which are explained the potential and SCH approximations (Appendix I), specific group theory and selection rules (Appendix II), the actual formulae for the EPME (Appendix III), and a description of the computer codes developed and used (Appendix IV).

CHAPTER II

FORMAL THEORY AND METHODS OF CALCULATION

2-1. Born-Oppenheimer Theory for Crystalline Solids

Crystalline solids, by definition, possess a definite periodic translational symmetry. Though the specific crystal structure is determined by minimization of the free energy, the various lattice symmetries inherent in a particular crystal structure frequently may be exploited to reduce the difficulty in carrying through whatever formal ansatz has been elected. Thus, the translational periodicity of a perfect crystal allows one to reduce many problems to considerations within a single cell by application of Bloch's theorem. Group theoretical methods also may be used to take explicit advantage of the crystal symmetry; as, for example, in the block diagonalization of secular matrices commonly done in energy band and molecular theory.

The elementary form of Bloch's theorem for a particle moving in a periodic potential $V(\underline{r})$ is[16]

$$\Psi_{\underline{k}}(\underline{r}+\underline{R}_n) = \exp[i\underline{k}\cdot\underline{R}_n]\Psi_{\underline{k}}(\underline{r}) \qquad (2\text{-}1)$$

$$V(\underline{r}+\underline{R}_n) = V(\underline{r}) \qquad (2\text{-}1a)$$

where $\Psi_{\underline{k}}(\underline{r})$ is the particle eigenfunction with wave vector $\underline{k}$ and energy $E_{\underline{k}}$, and $\underline{R}_n$ is any translation that leaves the solid or lattice invariant. The extension to multi-particle systems is straightforward.[16]

The symmetries characterizing a solid are valid only for a static crystal structure. In reality, the solid consists of moving nuclei whose motion is centered on the lattice sites. However, because the nuclei are bound in the crystal, they appear on the average to be at the equilibrium (i.e. static) lattice sites. It is then intuitively plausible (because of the smallness of the electron mass relative to the nuclear mass) to begin a treatment of electrons in a solid by assuming that the nuclei may be taken as fixed at the given lattice sites for a specified density. After a solution to this problem is achieved, the motion of the nuclei may be taken into account by a perturbative calculation of the electronic response. Just such an endeavor is the purpose of this research.

The formal basis for this kind of effort was first enunciated by Born and Oppenheimer[9] and the general theory has become known by their names. Following the notation of references 10, 16, and 17, the total solid Hamiltonian H is written as

$$\begin{aligned} H(\underline{R}) &= H_n(\underline{R}) + H_e(\underline{r},\underline{R}) \\ &= \Big(\sum_j p_j^2/2M + V_n(\underline{R})\Big) + \Big(\sum_i p_i^2 + V_{ne}(\underline{r},\underline{R}) + V_e(\underline{r})\Big) \qquad (2\text{-}2) \end{aligned}$$

where Rydberg atomic units will be employed throughout this work except as otherwise noted. In (2-2), M is the nuclear mass with the sum j over nuclei, the sum i is over electrons, $V_n(\underline{R})$ is the nuclear-nuclear interaction potential, $V_{ne}(\underline{r},\underline{R})$ is the nuclear-electron interaction potential, and $V_e(\underline{r})$ is the electron-electron interaction potential. Also $\underline{R}$ is a supervector of all nuclear position vectors and $\underline{r}$ plays a similar role for electrons. The grouping of the terms in (2-2) is suggestive of the role which the nuclear coordinates play as parameters in the adiabatic or instantaneous response theory of electronic structure. That is, the last three terms in (2-2) give the Schrödinger equation for the electronic state as

$$H_e(\underline{R})\Psi_{\underline{k}}(\underline{r},\underline{R}) = (\sum_i p_i^2 + V_{ne}(\underline{r},\underline{R}) + V_e(\underline{r}))\Psi_{\underline{k}}(\underline{r},\underline{R})$$
$$= E_{\underline{k}}(\underline{R})\Psi_{\underline{k}}(\underline{r},\underline{R}) \qquad (2\text{-}3)$$

with $E_{\underline{k}}(\underline{R})$ the total electronic energy of the $\underline{k}^{th}$ state dependent upon the nuclear coordinates $\underline{R}$ as parameters.

The electronic eigenfunctions of (2-3) form in general a complete basis set and therefore may be used to expand the total system (nuclear and electronic) wave function

$$\Xi(\underline{r},\underline{R}) = \sum_{\underline{k}} \Phi(\underline{k},\underline{R})\Psi_{\underline{k}}(\underline{r},\underline{R}) \qquad (2\text{-}4)$$

where the expansion coefficients depend on the $\underline{k}^{th}$ electronic state and the nuclear coordinates $\underline{R}$. Operating on (2-4) with the total Hamiltonian H (2-2) gives three terms

$$H\Xi(\underline{r},\underline{R}) = \sum_{\underline{k}}(\Psi_{\underline{k}}(\underline{r},\underline{R})[\sum_j p_j^2/2M + V_n(\underline{R}) + E_{\underline{k}}(\underline{R})]\Phi(\underline{k},\underline{R})$$
$$- 1/M\ \nabla_{\underline{R}}\Psi_{\underline{k}}(\underline{r},\underline{R})\cdot\nabla_{\underline{R}}\Phi(\underline{k},\underline{R}) - 1/2M\ \Phi(\underline{k},\underline{R})\nabla^2_{\underline{R}}\Psi_{\underline{k}}(\underline{r},\underline{R})\ ) \qquad (2\text{-}5)$$

By multiplying the last two terms in (2-5) by $\Psi^*_{\underline{k}'}(\underline{r},\underline{R})$ and integrating over the electronic coordinates, these terms may be shown[17-20] to be related to electronic scattering from the state $\underline{k}$ to $\underline{k}'$. Because this scattering is not in accordance with the adiabatic theory (which requires the electronic state be unchanged) and because the terms are small due to the factor of the nuclear mass, the last two terms may be eliminated from consideration.

Examination of the rest of (2-5) (after integration over the electronic coordinates and elimination of the non-adiabatic terms) shows that we have achieved a quite plausible separation between the nuclear and the electronic motions. This separation is emphasized by requiring that the $\Phi(\underline{k},\underline{R})$ be eigenfunctions of the nuclear motion determined from (2-5)

$$\left(H_n(\underline{R}) + E_{\underline{k}}(\underline{R}) \right) \Phi_{\underline{q}\lambda}(\underline{k},\underline{R}) = E_{\underline{q}\lambda}(\underline{R})\Phi_{\underline{q}\lambda}(\underline{k},\underline{R}) \qquad (2\text{-}6)$$

where, in the case of a lattice dynamical treatment,

$$E_{\underline{q}\lambda}(\underline{R}) = (n_{\underline{q}\lambda} + 1/2)\ \omega_{\underline{q}\lambda} \qquad (2\text{-}7)$$

$E_{\underline{q}\lambda}$ is the total energy of the n^{th} state for the $\underline{q}^{th}$ phonon of frequency ω and λ polarization.

The separation of the electronic and nuclear motion has been accomplished by use of the adiabatic hypothesis. The nuclear motion governed by (2-6) may now be described as a phonon field either of the ordinary harmonic type or the intrinsically quantum mechanical type given by SCH theory (see Appendix I). Both approaches diagonalize a force constant or dynamical matrix to obtain the phonon eigenvalues. The only difference is in the determination of the dynamical matrix (a matrix of self-consistently averaged second derivatives in the SCH theory as opposed to equilibrium values in plain harmonic theory).

The quantum parameter Λ^2 introduced in Appendix I is a measure of the quantum mechanical character (or zero point motion) of a system. Of the two rare gas solids considered here, the value of Λ for argon is fairly small, while that for neon indicates somewhat more substantial zero point motion.[21] Therefore the unperturbed (*i.e.* adiabatic) phonon spectra of argon and neon have been calculated by the SCH theory.

As is well known, the principal difficulty in solving the adiabatic electronic structure problem (2-3) arises from the many-body nature of the electron-electron interaction combined with the requirement that the electronic wave functions be properly anti-symmetrized. Almost all treatments have as their aim the construction of a one-electron model in which the electrons are treated as independent particles moving in some well-defined average field due to all the other electrons. Even at this level, rigorous treatment of Fermi statistics introduces complicated exchange contributions to the effective Hamiltonian. The inclusion of spatial correlation introduces further complications. The net effect is to make the problem almost intractable for a crystal. For example, correlation and exchange effects may be treated through a computational realization of the configuration interaction scheme for atoms and molecules, but in solids such an approach is, to this date, well beyond the limits of feasibility and other schemes must be invoked.[22] A much explored alternative is to make some sacrifice in rigor (small, one hopes) and thereby obtain a soluble model of electron behavior. The next section deals with the form of such a model and the Hamiltonian $H_e(\underline{R})$ of (2-3) that results, with particular emphasis on the features needed to achieve the eventual goal of this work.

2-2. The Xα Hamiltonian

A brief outline of the Xα method for the non-spin polarized case will be given here. The method itself is well documented and has had many useful applications in a variety of circumstances.[12] For the present purposes, the method allows a computationally manageable form for the Hamiltonian in calculations of the electronic properties of a solid.

For a static lattice, in the adiabatic sense, the Xα method assumes for the total electronic energy the expression

$$\langle E_{X\alpha} \rangle = \langle T_{X\alpha} \rangle + \langle U_{X\alpha} \rangle \qquad (2\text{-}8)$$

where

$$\langle T_{X\alpha}\rangle = -\sum_i n_i \int u_i^*(1)\nabla_1^2 u_i(1)\,d\underline{r}_1 \tag{2-9}$$

$$\langle W_{X\alpha}\rangle = \sum_{jm}{}' Z_j Z_m/R_{jm} - \sum_j \int \rho(1)(2Z_j/r_{1j})\,d\underline{r}_1 + \int \rho(1)(\rho(2)/r_{12})\,d\underline{r}_{12}$$

$$+ 1/2 \int \rho(1)U_{X\alpha}(1)\;d\underline{r}_1 \tag{2-10}$$

with Z_j denoting the jth nuclear charge and R_{jm} the jth and mth nuclear separation. The charge density is

$$\rho(1) = \sum_i n_i u_i^*(1)u_i(1) \tag{2-11}$$

with n_i the occupancy of the spin orbital u_i. The local exchange-correlation operator in the non-spin polarized case is defined as

$$U_{X\alpha}(1) = -9\alpha(3/8\pi\;\rho(1))^{1/3} \tag{2-12}$$

with α a parameter to be calibrated against, for example, atomic properties. Application of the variational principle to (2-8) leads to the effective one-electron Schrödinger equation

$$[-\nabla_1^2 + \sum_j Z_j/r_{1j} + \int (2Z_1/r_{12})\rho(2)\,d\underline{r}_2 - 6\alpha(3/8\pi\;\rho(1))^{1/3}]u_i(1) = E_i u_i(1) \tag{2-13}$$

The one-electron eigenvalues E_i of (2-13) are related to the occupancies n_i so that Fermi statistics are obeyed.

The static lattice cohesive energy per particle for a solid of N constituent nuclear particles and of a specified density is defined as

$$(E/N) = \langle E_{X\alpha}\rangle_{solid}/N - \langle E_{X\alpha}\rangle_{atom} \tag{2-14}$$

This definition is consistent with Appendix I provided the two Xα total energies are calculated at the same α.

The selection of a value for α has been the subject of much investigation and discussion. However, as a result of previous calculations done on argon[23] and neon,[24] a value of 2/3 has been used for neon and a value of 0.72131 for argon. The neon value is that due to Gaspar, Kohn, and Sham,[25] while the argon value is such that the virial theorem is satisfied for the energies determined from a single determinant of argon $X\alpha$ orbitals using that value of α.[26]

2-3. The APW Method

The APW method is a well-established scheme for solving a given one-electron eigenvalue problem for a crystal. An excellent review by Mattheiss *et al.*[3] discusses the self-consistent field symmetrized form of the APW method (SAPW). Just this form has been used in the present research. Therefore the presentation here will follow the notation and style of that review. As the calculation was done on two solids which have the same symmorphic space group (see Appendix I), the explicit reference[3] to non-primitive lattice translations will be dropped.

The potential, of the functional form discussed in section (2-2), is assumed to be spherically symmetric inside spheres centered at each nuclear site in a solid and constant outside those spheres. This periodic muffin-tin (MT) potential is a physically plausible one which approximates the exact periodic potential while being much more convenient. In the constant potential region, the APW basis functions are taken to be plane waves; while inside the sphere the APW basis functions are expanded in spherical harmonics and energy dependent radial functions.

The electronic Bloch function for the j^{th} band and $\underline{k}^{th}$ wave vector with energy $E_j(\underline{k})$ may be expanded in terms of these APW basis functions

$$\Psi_{j\underline{k}}(\underline{r}) = \sum_{\underline{K}} C(\underline{K})\Phi(\underline{k}+\underline{K},\underline{r},E_j) \tag{2-15}$$

with the sum $\underline{K}$ over all reciprocal lattice vectors. The APW basis function of (2-15) is, letting R_s be the MT sphere radius,

$$\Phi(\underline{k}+\underline{K},\underline{r},E_j) = \exp[i(\underline{k}+\underline{K})\cdot\underline{r}] \qquad r>R_s \tag{2-16a}$$

$$= \sum_{\ell}\sum_{m} 4\pi i^{\ell}\frac{j_\ell(|\underline{k}+\underline{K}|R_s)}{u_\ell(R_s,E_j)}\, Y^*_{\ell m}(\theta_{\underline{k}+\underline{K}},\phi_{\underline{k}+\underline{K}})\, u_\ell(r,E_j)Y_{\ell m}(\theta,\phi) \qquad r<R_s \tag{2-16b}$$

In (2-16b), $Y_{\ell m}$ is a spherical harmonic (and is of the Condon and Shortley convention[27]), j_ℓ is a spherical Bessel function, $\theta_{\underline{k}+\underline{K}}$ and $\phi_{\underline{k}+\underline{K}}$ are the angular coordinates of the vector $\underline{k}+\underline{K}$, E_j is the energy eigenvalue of the j^{th} band and $\underline{k}^{th}$ wave vector and the $u_\ell(r,E_j)$ are solutions to the radial Schrödinger equation (in Rydberg units)

$$-1/r^2\, d/dr\,(r^2\, du_\ell/dr) + [(\ell(\ell+1)/r^2) + V_{MT}]\, u_\ell = E_j u_\ell \tag{2-17}$$

where V_{MT} is the muffin-tin potential.

The Bloch function of the j^{th} band and $\underline{k}^{th}$ wave vector can be symmetrized to transform irreducibly as the n^{th} basis partner of the α^{th} representation of the group of $\underline{k}$. First, projection operators are applied to the APW basis functions of (2-16) to obtain the the SAPW basis functions

$$\phi^{\alpha}_{n,s}(\underline{k}+\underline{K},\underline{r},E^{\alpha}) = \sum_{\underline{R}\varepsilon G_{\underline{k}}} \Gamma^{*\alpha}_{n,s}(\underline{R})\underline{R}\Phi(\underline{k}+\underline{K},\underline{r},E_j) \tag{2-18}$$

with $\Gamma^*_{n,s}$ the n^{th} and s^{th} element of the α^{th} matrix representation of $\underline{R}$, and $\underline{R}$ belonging to the operations of the group of $\underline{k}$ $(G_{\underline{k}})$. Then, with these SAPW, the symmetrized Bloch functions are obtained

$$\Psi^{\alpha}_{n\underline{k}}(\underline{r}) = \sum_{\underline{K}}\sum_{s} C^{\alpha}_{n,s}(\underline{K})\phi^{\alpha}_{n,s}(\underline{k}+\underline{K},\underline{r},E^{\alpha}) \tag{2-19}$$

with E^{α} in both (2-18) and (2-19) the energy eigenvalue of the α^{th}

representation. Strictly speaking, this eigenvalue should have a basis partner index, but for most cases (as in the present calculation) the eigenvalue is degenerate in the basis partner index.[3]

The effect of a rotation operation $\underline{R}$ on the APW basis function (2-16) is defined by

$$\begin{aligned} \underline{R}\,\Phi(\underline{k},\underline{r},E_j) &= \Phi(\underline{k},\underline{R}^{-1}\underline{r},E_j) \\ &= \Phi(\underline{Rk},\underline{r},E_j) \qquad (2\text{-}20) \end{aligned}$$

with $\underline{R}^{-1}$ the inverse operation to $\underline{R}$. The final form of the SAPW becomes

$$\Phi^{\alpha}_{n,s}(\underline{k}+\underline{K}.\underline{r},E^{\alpha}) = \sum_{\underline{R}\in G_{\underline{k}}} \Gamma^{*\alpha}_{n,s}(\underline{R})\ \exp[i\underline{Rk}\cdot\underline{r}] \qquad r>R_s \quad (2\text{-}21)$$

$$= \sum_{\underline{R}\in G_{\underline{k}}} \Gamma^{*\alpha}_{n,s}(\underline{R}) \sum_{\ell}\sum_{m} 4\pi i^{\ell}\frac{j_{\ell}(kR_s)}{u_{\ell}(E^{\alpha},R_s)}\, Y^{*}_{\ell m}(\theta_{\underline{Rk}},\varphi_{\underline{Rk}})\ u_{\ell}(E^{\alpha},r)Y_{\ell m}(\theta,\phi) \quad r<R_s \quad (2\text{-}22)$$

where on the RHS of both (2-21) and (2-22)

$$\underline{Rk} \equiv \underline{R}(\underline{k}+\underline{K}) \text{ and } k \equiv |\underline{Rk}| \equiv |\underline{R}(\underline{k}+\underline{K})| \qquad (2\text{-}23)$$

In most applications using the APW basis, the addition theorem of the spherical harmonics (A3-12) may be invoked to further simplify (2-22)

$$\Phi^{\alpha}_{n,s}(\underline{k}+\underline{K},\underline{r},E^{\alpha}) = 4\pi \sum_{\underline{R}\in G_{\underline{k}}} \Gamma^{*\alpha}_{n,s}(\underline{R}) \sum_{\ell} i^{\ell}\,\frac{j_{\ell}(kR_s)}{u_{\ell}(E^{\alpha},R_s)}\, P_{\ell}\!\left(\frac{\underline{Rk}\cdot\underline{r}}{kr}\right) u_{\ell}(E^{\alpha},r) \quad (2\text{-}24)$$

The purpose of this symmetrization is two-fold: the reduction of the size of the secular matrix to be solved, and clear identification of the contributing symmetry to the electronic bands. As a consequence of using SAPWs , the entire problem must be formulated in symmetrized terms. This means that the phonons of the nuclear motion for the electron-phonon interaction considered here must be expressed in terms of the appropriate irreducible representations and basis partner (which is equivalent to the phonon wave vector and polarization). The results of the symmetrization of the phonons (in the form of their dispersion curves) are given in Figure 2-1 for the typical fcc solid with one atom per unit cell. In Table 2-1 are given the eigenvectors of the phonons at each of the symmetry points and at each polarization (or basis partner).

One final point of the APW method concerns normalization. Proper normalization is required if the electronic Bloch functions are to be used outside of the actual SAPW program. The normalization integral of (2-19) is, in general, over the entire periodic macro-cell; however, using Bloch's theorem the integral may be reduced to N times the integral over a single unit cell (where N is the number of unit cells in the periodic volume). Reference 3 shows that the application of standard group theoretical methods gives for the normalization

$$\int \Psi^{*\alpha}_{n\underline{k}}(\underline{r})\Psi^{\alpha}_{n\underline{k}}(\underline{r})d\underline{r} = N\ (g/d_{\alpha}) \sum_{\underline{K}'} \sum_{\underline{K}} \sum_{\underline{R}\varepsilon G_{\underline{k}}} \Gamma^{*\alpha}_{n,n}(\underline{R})[\Omega\delta_{\underline{Rk}',\underline{k}+\underline{K}} -$$

$$4\pi R_s^2 \frac{j_\ell(|\underline{Rk}'-(\underline{k}+\underline{K})|R_s)}{|\underline{Rk}'-(\underline{k}+\underline{K})|R_s} + 4\pi\sum_{\ell}(2\ell+1)\frac{j_\ell(k'R_s)\ j_\ell(kR_s)}{u^*_\ell(E^\alpha,R_s)u_\ell(E^\alpha,R_s)}\int_o^{R_s} u^*_\ell u_\ell r^2 dr] \quad (2\text{-}25)$$

where g is the order $G_{\underline{k}}$, d_α is the dimensionality of the α^{th} representation, and Ω is the primitive unit cell volume. The notation of (2-23) has been used in (2-25) and in Appendix III where the formulae for the EPME are derived based on the SAPW in the form (2-22).

2-4. The Fröhlich Hamiltonian

Though Fröhlich[4,28] and many others[19] using his approach had the principal objective of explaining metallic superconductivity, the Hamiltonian and approach to the electron-phonon interaction which he formulated is of a general nature (within, of course, certain approximations) and

Figure 2-1. Prototype fcc rare gas crystal phonon dispersion curves. Wave vector representation labels and first BZ symmetry direction labels are from ref. 29 . Dotted lines indicate symmetry points on the zone boundaries. Symmetry directions between these points are denoted by a label and a three component vector with values of x from 0 to 1. The frequency units are typically in the range from 0 to 10 THz (10^{12}Hz).

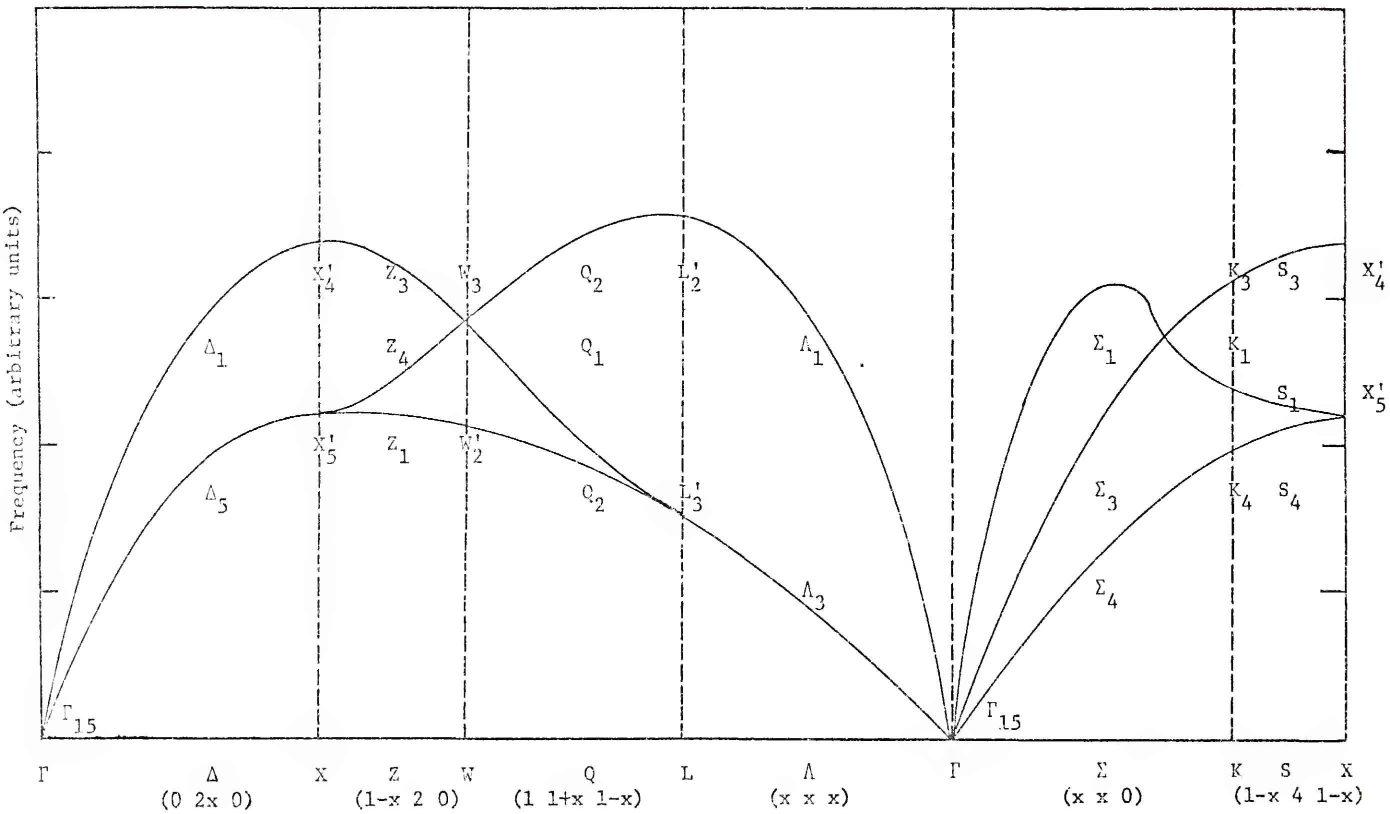
Frequency (arbitrary units)
Γ
Δ
(0 2x 0)
X
Z
(1-x 2 0)
W
Q
(1 1+x 1-x)
L
Λ
(x x x)
Γ
Σ
(x x 0)
K
S
X
(1-x 4 1-x)
Γ_{15}
Δ_1
Δ_5
X'_4
X'_5
Z_3
Z_4
Z_1
W_3
W'_2
Q_2
Q_1
Q_2
L'_2
L'_3
Λ_1
Λ_3
Γ_{15}
Σ_1
Σ_3
Σ_4
K_3
K_1
K_4
S_3
S_1
S_4
X'_4
X'_5

Table 2-1

Phonon Eigenvectors of the Six Non-equivalent BZ Points

Symmetry Point	Matrix Form of Eigenvector[a]		
	L	T1	T2
Γ	1	0	0
	0	1	0
	0	0	1
Δ	0	$\frac{-1i}{\sqrt{2}}$	$\frac{-1i}{\sqrt{2}}$
	i	0	0
	0	$\frac{1}{\sqrt{2}}$	$\frac{-1}{\sqrt{2}}$
X	0	$\frac{-1i}{\sqrt{2}}$	$\frac{1i}{\sqrt{2}}$
	1	0	0
	0	$\frac{1}{\sqrt{2}}$	$\frac{1}{\sqrt{2}}$
Σ	$\frac{1i}{\sqrt{2}}$	$\frac{1i}{\sqrt{2}}$	0
	$\frac{1i}{\sqrt{2}}$	$\frac{-1i}{\sqrt{2}}$	0
	0	0	i
L	$\frac{1}{\sqrt{3}}$	$\frac{1}{2} - \frac{1i}{\sqrt{12}}$	$\frac{1}{2} + \frac{1i}{\sqrt{12}}$
	$\frac{1}{\sqrt{3}}$	$\frac{-1}{2} - \frac{1i}{\sqrt{12}}$	$\frac{-1}{2} + \frac{1i}{\sqrt{12}}$
	$\frac{1}{\sqrt{3}}$	$\frac{1i}{\sqrt{3}}$	$\frac{-1i}{\sqrt{3}}$
W[b]	0	0	i
	$\frac{1}{2} - \frac{1i}{2}$	$\frac{-1}{2} - \frac{1i}{2}$	0
	$\frac{1}{2} + \frac{1i}{2}$	$\frac{-1}{2} + \frac{1i}{2}$	0

[a] Row denotes x, y, z components; column denotes polarization (L longitudinal; T1 and T2 transverse 1 and 2); $i = \sqrt{-1}$

[b] The first two eigenvectors of W are actually pseudo-longitudinal and the last is actually pseudo-transverse.

will be utilized in this work. An excellent paper by Hedin and Lundqvist[30] (the author is grateful to Dr. N.Y. Öhrn for bringing this reference to his attention) gives a strictly formal justification for the assumed form of the Fröhlich Hamiltonian that has been used here. The purpose here is to present that assumed form within certain approximations and show the natural connection to the Born-Oppenheimer Hamiltonian.

As a convenient starting point, the Hamiltonian H of (2-2), for N nuclei of mass M, is expanded about the equilibrium lattice sites ($\underline{R}^o$) in powers of the displacements ($\delta\underline{R}$). In keeping with the harmonic model, the gradient of the total energies of the electrons and of the nuclei taken together vanishes. The only terms left to first order in the displacements are the electron-electron and nuclear-electron interactions

$$\begin{aligned} H(\underline{R}^o) &= H_n(\underline{R}^o) \quad + \quad H_e(\underline{R}^o) \quad + \quad H_{EP} \\ &= [T_n(\underline{R}^o)+V_n(\underline{R}^o)] + [T_e(\underline{R}^o)+V_e(\underline{R}^o)+V_{ne}(\underline{R}^o)] + \delta\underline{R}\cdot\nabla_{\underline{R}}(V_{ne}+V_e)\big|_{\underline{R}^o} \qquad (2\text{-}26) \end{aligned}$$

H_{EP} is the electron-phonon interaction to first order in the displacement and by an obvious simplification of (2-2), T has replaced the kinetic energy sums. The individual operators of (2-26) may be expressed (see, for instance, references 22 and 31) in second quantized field operator form as

$$\begin{aligned} H_n(\underline{R}^o) &= \sum_{\underline{q}\lambda} E^o_{\underline{q}\lambda} a^{\dagger}_{\underline{q}\lambda} a_{\underline{q}\lambda} \\ &= \sum_{\underline{q}\lambda} (n_{\underline{q}\lambda} + 1/2)\, \omega^o_{\underline{q}\lambda} \qquad (2\text{-}27) \end{aligned}$$

with the a's denoting boson quasi-particle operators,

$$H_e(\underline{R}^o) = \sum_{\underline{k}} E^o_{\underline{k}}\, c^{\dagger}_{\underline{k}} c_{\underline{k}}$$

$$= \sum_{\underline{k}} n_{\underline{k}} E^{o}_{\underline{k}} \tag{2-28}$$

with the c's denoting fermi quasi-particle operators, and

$$H_{EP} = \sum_{\underline{k},\underline{k}'} M(\underline{k}';\underline{k}) c^{\dagger}_{\underline{k}'} c_{\underline{k}} (a^{\dagger}_{-\underline{q}\lambda} + a_{\underline{q}\lambda}) \tag{2-29}$$

In (2-29), the sum is restricted to $\underline{q} = \underline{k}' - \underline{k} + \underline{K}$ ($\underline{K}$, a reciprocal lattice vector), the displacements have been expressed in normal mode coordinates[1,22]

$$\begin{aligned} \delta\underline{R}_j &= (NM)^{-1/2} \sum_{\underline{q}\lambda} Q_{\underline{q}\lambda} \exp[i\underline{q}\cdot\underline{R}^{o}_{j}]\underline{\varepsilon}_{\underline{q}\lambda} \\ &= (NM)^{-1/2} \sum_{\underline{q}\lambda} (2\omega^{o}_{\underline{q}\lambda})^{-1/2} (a^{\dagger}_{-\underline{q}\lambda} + a_{\underline{q}\lambda}) \end{aligned} \tag{2-30}$$

and the electron-phonon matrix element (EPME) [between electronic Bloch states (2-3)] is defined as

$$\begin{aligned} M(\underline{k}';\underline{k}) &= \langle\psi^{o}_{\underline{k}'}|H_{EP}|\psi^{o}_{\underline{k}}\rangle \\ &= (NM2\omega^{o}_{\underline{q}\lambda})^{-1/2} \langle\psi^{o}_{\underline{k}'}|\underline{\varepsilon}_{\underline{q}\lambda}\cdot\nabla_{\underline{R}}(V_{ne}+V_{e})|_{\underline{R}^{o}}|\psi^{o}_{\underline{k}}\rangle \end{aligned} \tag{2-31}$$

The energies of equations (2-27) and (2-28) have the same meaning as those of (2-3) and (2-7) and the superscript o means the static equilibrium lattice (unperturbed).

The totality of (2-27), (2-28), and (2-29) comprise the assumed form for the Fröhlich Hamiltonian H_F used in this work

$$H_F = \sum_{\underline{k}} E^{o}_{\underline{k}} c^{\dagger}_{\underline{k}} c_{\underline{k}} + \sum_{\underline{q}\lambda} E^{o}_{\underline{q}\lambda} a^{\dagger}_{\underline{q}\lambda} a_{\underline{q}\lambda} + \sum_{\underline{k},\underline{k}'} M(\underline{k}';\underline{k}) c^{\dagger}_{\underline{k}'} c_{\underline{k}} (a^{\dagger}_{-\underline{q}\lambda} + a_{\underline{q}\lambda}) \tag{2-32}$$

Some explanation of these equations is now in order. In (2-28) and (2-29), the $\underline{k}$ and $\underline{k}'$ also imply band indices. Bra and ket notation simplify the electronic coordinate integration in (2-31). The Bloch condition of (2-1) has been used in (2-31) to remove the exponential of (2-30) and to give the selection rule

$$\underline{q} = \underline{k}' - \underline{k} + \underline{K} \tag{2-33}$$

which governs the sum restrictions in (2-29) and (2-32). The presence of the reciprocal vector $\underline{K}$ allows for umklapp processes.[16,19] The convention of the wave vectors throughout this work is based on (2-33) with $\underline{k}$ denoting the initial state (valence or "p-like" band), $\underline{k}'$ the final state (conduction or "s-like" band), and $\underline{q}$ the phonon wave vector.

The eigenvectors and normal mode amplitudes of (2-30) are chosen to have the following phase convention

$$Q^*_{\underline{q}\lambda} = Q_{-\underline{q}\lambda} \tag{2-34a}$$

$$\underline{\varepsilon}_{\underline{q}\lambda} = \underline{\varepsilon}_{-\underline{q}\lambda} \tag{2-34b}$$

The eigenvectors for the symmetry points used in this work (see Appendix I) were given in the previous section (Table 2-1) and have been adapted in symmetrized form to the present calculation from those vectors of reference 32. These eigenvectors are seen to satisfy the following orthogonality and closure relations

$$\underline{\varepsilon}_{\underline{q}\lambda} \cdot \underline{\varepsilon}_{\underline{q}\lambda'} = \delta_{\lambda\,\lambda'} \tag{2-35a}$$

$$\sum_{\lambda} \varepsilon^{i}_{\underline{q}\lambda}\, \varepsilon^{j}_{\underline{q}\lambda} = \delta_{i,j} \tag{2-35b}$$

with i,j the x, y, or z component of the eigenvector.

In writing down H_I of (2-32), the explicit electron-electron and electron-nuclear interactions are accounted for by using an appropriate screened form of the potentials in the EPME expression (2-31) and by calculating the "bare" or unperturbed phonons of the Hamiltonian H_F using some method that gives the correct small wavenumber behavior of the phonon energies (i.e. proportional to the wavenumber). The screening is inherent in the Xα potential approximation for exchange and correlation effects and the correct behavior of the phonon energies is contained in the SCH theory if any reasonable (though not necessarily accurate) total lattice potential (in this work, the Lennard-Jones superposition) is used to calculate the unperturbed phonon spectra. Therefore, as used here, the bose and fermi creation and annihilation operators of (2-27) and (2-28) are formally "quasi-particle" operators as opposed to the usual single-particle electron or phonon operators. This point is emphasized and given a strictly formal justification by Hedin and Lundqvist.[30] H_F, in the form of (2-32), therefore will be assumed to be applicable to the present calculation. It should be mentioned, however, that energy corrections calculated using H_F have been found to affect only electrons close to the Fermi surface, while the phonon dispersion was altered substantially.[30,32] These facts will be used both as an aid and as a check for this calculation.

By means of H_F, the energy corrections may be calculated using second order Rayleigh-Schrödinger perturbation theory. First, we define some quantities for purposes of simplification

$$H^o = H_n(\underline{R}^o) + H_e(\underline{R}^o)$$

$$= \sum_{\underline{q}} E^o_{\underline{q}} a^\dagger_{\underline{q}} a_{\underline{q}} + \sum_{\underline{k}} E^o_{\underline{k}} c^\dagger_{\underline{k}} c_{\underline{k}} \tag{2-36}$$

$$E^o = \sum_{\underline{q}} E^o_{\underline{q}} n_{\underline{q}} + \sum_{\underline{k}} E^o_{\underline{k}} n_{\underline{k}} \tag{2-37}$$

where the polarization label is implicit in $\underline{q}$ as is the band index in $\underline{k}$, and $n_{\underline{k}}$ and $n_{\underline{q}}$ denote the occupation numbers of the electronic state $\underline{k}$ and phonon state $\underline{q}$ respectively. It should be noted that the electronic occupation numbers have an implicit spin summation factor of two contained in them and that both the phonon and electronic occupation numbers are not necessarily integers because of the "quasi-particle" nature of the field operators. The total energy to second order in the perturbation H_{EP} may now be written as[31]

$$E = E^{o} + <\Xi|H_{EP}|\Xi> + <\Xi|H_{EP}(E^{o} - H^{o})^{-1}H_{EP}|\Xi> \qquad (2\text{-}38)$$

where bra and ket notation indicate nuclear and electronic integration and Ξ is the ground state total system wave function [in the sense of section 2-1 and (2-4)] with $n_{\underline{k}}$ electrons in state $\underline{k}$ and $n_{\underline{q}}$ phonons in state $\underline{q}$. The first order energy term in (2-38) vanishes due to the harmonic nature of the phonons (formally this is equivalent to the creation or destruction of a phonon in the total system and the resulting orthogonality of that system state to the system ground state). The total second order energy correction of (2-38) may be shown to be[31]

$$\begin{aligned} E^{(2)} = <\Xi|\sum_{\underline{k},\underline{k}'}|M(\underline{k}';\underline{k})|^{2}[a^{\dagger}_{-\underline{q}}c^{\dagger}_{\underline{k}}c_{\underline{k}'}(E^{o}-H^{o})^{-1}a_{-\underline{q}}c^{\dagger}_{\underline{k}'}c_{\underline{k}} \\ + a^{\dagger}_{\underline{q}}c^{\dagger}_{\underline{k}}c_{\underline{k}'}(E^{o}-H^{o})^{-1}a_{\underline{q}}c^{\dagger}_{\underline{k}'}c_{\underline{k}}]|\Xi> \qquad (2\text{-}39) \end{aligned}$$

where the sum is restricted by (2-33). For clarity and illustration, Figure 2-2 shows the interactions inherent in the assumed form of H_{EP} and the processes that contribute to the total second order energy of (2-39). The use of (2-36) and (2-37) in terms of occupation numbers reduces (2-39) to

$$E^{(2)} = \sum_{\underline{k},\underline{k}'}|M(\underline{k}';\underline{k})|^{2}n_{\underline{k}'}(1-n_{\underline{k}})\left[\frac{n_{-\underline{q}}}{E^{o}_{\underline{k}}-E^{o}_{\underline{k}'}+\omega^{o}_{-\underline{q}}} + \frac{(n_{\underline{q}}+1)}{E^{o}_{\underline{k}}-E^{o}_{\underline{k}'}-\omega^{o}_{\underline{q}}}\right] \qquad (2\text{-}40)$$

where, again, the sum is restricted by (2-33). The symmetry of the eigenvectors (2-34b) gives $\omega^{o}_{\underline{q}} = \omega^{o}_{-\underline{q}}$; thus in thermal equilibrium, it is expec-

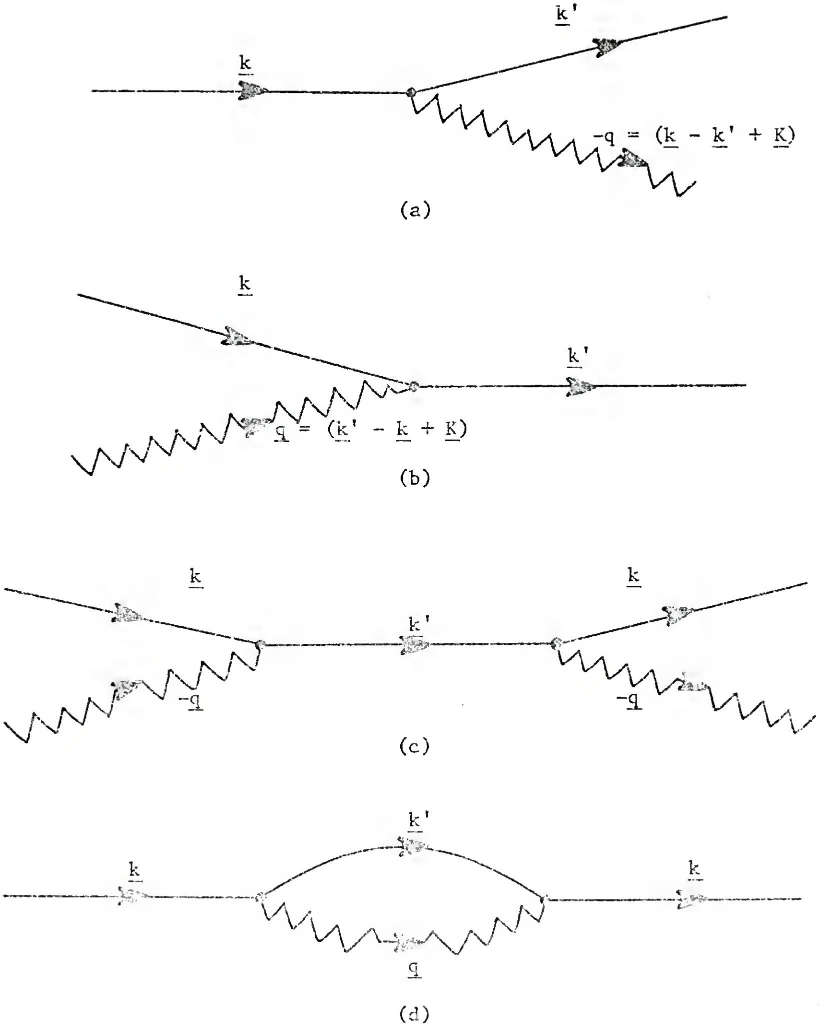

Figure 2-2. Illustration of the interactions involved in the perturbation Hamiltonian H_{EP} and of the resultant second order energy processes. The various pictures and their corresponding terms are:

(a) H_{EP} $a^{\dagger}_{-\underline{q}} c^{\dagger}_{\underline{k}'} c_{\underline{k}}$ (b) H_{EP} $c^{\dagger}_{\underline{k}'} c_{\underline{k}} a_{\underline{q}}$

(c) $E^{(2)}$ $a^{\dagger}_{-\underline{q}} c^{\dagger}_{\underline{k}} c_{\underline{k}'} c^{\dagger}_{\underline{k}'} c_{\underline{k}} a_{-\underline{q}}$ (d) $E^{(2)}$ $c^{\dagger}_{\underline{k}} c_{\underline{k}'} a_{\underline{q}} a^{\dagger}_{\underline{q}} c^{\dagger}_{\underline{k}'} c_{\underline{k}}$

ted that $n_{\underline{q}} = n_{-\underline{q}}$. Therefore, (2-40) may be simplified to

$$E^{(2)} = \sum_{\underline{k},\underline{k}'} |M(\underline{k}';\underline{k})|^2 n_{\underline{k}'} \left[\frac{2n_{\underline{q}}(E^{o}_{\underline{k}'}-E^{o}_{\underline{k}})}{(E^{o}_{\underline{k}}-E^{o}_{\underline{k}'})^2-\omega^{o2}_{\underline{q}}} + \frac{(1-n_{\underline{k}})}{E^{o}_{\underline{k}}-E^{o}_{\underline{k}'}-\omega^{o}_{\underline{q}}}\right] \qquad (2\text{-}41)$$

(2-41) is the total second order energy correction to the system and the electron-phonon effect on the phonons is in the term proportional to the phonon occupation $n_{\underline{q}}$.

Identification of the phonon perturbation with the total energy E of (2-38) necessary to increase the $\underline{q}^{th}$ phonon occupation by $n_{\underline{q}}$ gives[31]

$$\begin{aligned}\omega_{\underline{q}\lambda} &= \frac{\partial E}{\partial n_{\underline{q}\lambda}}\\ &= \omega^{o}_{\underline{q}\lambda} + \sum_{\underline{k}'} |M(\underline{k}';\underline{k})|^2 \left[\frac{2n_{\underline{k}'}(E^{o}_{\underline{k}'}-E^{o}_{\underline{k}})}{(E^{o}_{\underline{k}}-E^{o}_{\underline{k}'})^2-\omega^{o2}_{\underline{q}\lambda}}\right] \qquad (2\text{-}42)\end{aligned}$$

with the sum over $\underline{k}'$ still restricted by (2-33) and the polarization explicitly included as a reminder that the transitions are between representations of the wave vectors. For this calculation, the sum over $\underline{k}'$ is only over available scattered states in the conduction or excited bands. Expression (2-42) has been programmed (see Appendix IV) to calculate the total second order energy corrections only for transitions involving all "p-like" filled valence band states to all excited empty "s-like" conduction band states. These transitions are based on the selection rules calculated in Appendix II between the electron wave vector representations and the phonon wave vector representations.

2-5. The Derivation of the Form for the EPME

In section (2-4), the existence of an EPME was established and shown to follow as a natural consequence of the Born-Oppenheimer theory and was used in the Fröhlich Hamiltonian to calculate second order energy corrections to the phonons. The purpose of this section is to derive and justify an explicit form of the EPME specific to the APW formalism.

The muffin-tin (MT) potentials are assumed to move rigidly with the nuclei. This assumption is similar to the "rigid ion" approximation,[13] the fundamental, and physically more reasonable, distinction being that the MT potentials are a self-consistent description of the Born-Oppenheimer solid rather than a simple superposition of atomic potentials. Because the MT spheres are traditionally chosen to touch so as to maximize the fraction of the cell volume they enclose, there appears to be a problem of overlapping and mixing of adjacent potentials when the MTs are displaced (a point originally emphasized to the author[33]). Kenney[34] has stated that the validity and applicability of the APW method are rather independent of the sphere radius provided the sphere remains within the Wigner-Seitz cell (primitive unit cell). He also gives a plausible argument, in the case of metals, that the sphere radius be reduced five to ten percent from half the nearest neighbor distance. Ziman[16] devotes a considerable discussion to the effects of large displacements (small wavenumber) which is really only pertinent to metals or semi-conductors. Estimates, based on Kenney's suggestion, of the mean square displacement (in Rydberg atomic units)

$$(\Delta x)^2 = 1/(M\omega_D^2) \qquad (2\text{-}43)$$

for neon and argon show that the average displacements are about fifteen percent for neon and about ten percent for argon. In spite of this, and due to the fact that Ziman and Keaney consider large displacements only for metals, the overlap effect has been neglected. Both the smallness and the flatness (small derivative) of the potential in the overlap region (as contrasted to metals) tend to make this approximation plausible.

Following Golibersuch,[1] the Bloch function for the j^{th} band at the $\underline{k}^{th}$ wave vector in the perturbed lattice (i.e. perturbed by the electron-phonon interaction) is given approximately by first order perturbation theory as

$$\Psi_{\underline{k}} \simeq \Psi^{o}_{\underline{k}} + \sum_{\underline{k}'} \frac{M(\underline{k}';\underline{k})}{E^{o}_{\underline{k}}-E^{o}_{\underline{k}'}} \Psi^{o}_{\underline{k}'} \qquad (2\text{-}44)$$

with the band indices implicit (as in section 2-4) in the wave vector and with the summation in general over all states including core and valence (occupied) and conduction and excited (unoccupied). The superscript o will denote throughout this section the unperturbed static equilibrium lattice, while its absence will denote the perturbed lattice. The explicit $\underline{r}$ dependence and the band index j of section 2-3 will be dropped henceforth (except where essential for clarity) with the convention that the wave vector includes the band labeling. The square of $M(\underline{k}';\underline{k})$ is formally the first order (in the wave function) transition probability between the equilibrium states $\underline{k}$ and $\underline{k}'$ where, as in section 2-4, $\underline{k}$ is the initial state and $\underline{k}'$ the final state. It is therefore appropriate to take this quantity as the EPME. From the viewpoint of scattering, the EPME can be related to that part of the transition matrix (T matrix) linear in the nuclear displacement.

The static unperturbed Bloch functions, simplified and superscriven from (2-15), become

$$\Psi^o_{\underline{k}} = \sum_{\underline{K}} C^o(\underline{k},\underline{k}+\underline{K})\Phi^o(\underline{k}+\underline{K}) \qquad (2\text{-}45)$$

where the coefficients now contain an explicit reference to the initial state wave vector $\underline{k}$. This explicit reference is to remind us that the perturbed wave function, constructed from the perturbed APW basis functions, is not necessarily a periodic function

$$\Psi_{\underline{k}} = \sum_{\underline{K}} C(\underline{k},\underline{k}+\underline{K})\Phi(\underline{k}+\underline{K}) + \sum_{\underline{k}'\neq\underline{k}+\underline{K}} C(\underline{k},\underline{k}')\Phi(\underline{k}') \qquad (2\text{-}46)$$

where the $\underline{k}$ label on the LHS is only to indicate the initial eigenstate of the system.

In (2-46), all possible wave vectors are needed due to the non-periodic nature of the perturbed wave function; that is, the label $\underline{k}$ no longer denotes eigenstates of the now perturbed system. Expanding the perturbed APW basis functions and coefficients of (2-46) to first order in the nuclear displacements gives

$$C(\underline{k},\underline{k}+\underline{K}) = C^o(\underline{k},\underline{k}+\underline{K}) + \delta\underline{R}\cdot\nabla_{\underline{R}}C\Big|_{\underline{R}^o} \qquad (2\text{-}47)$$

$$\Phi(\underline{k}+\underline{K}) = \Phi^o(\underline{k}+\underline{K}) + \delta\underline{R}\cdot\nabla_{\underline{R}}\Phi\Big|_{\underline{R}^o} \qquad (2\text{-}48)$$

where $\delta\underline{R}$ are the displacements, $\nabla_{\underline{R}}$ are the gradients with respect to the nuclear coordinates, and $\underline{R}^o$ are the equilibrium configuration.

Using (2-47) and (2-48) in (2-46), and keeping only constant and linear terms

$$\Psi_{\underline{k}} \simeq \sum_{\underline{K}} C^o(\underline{k},\underline{k}+\underline{K})\Phi^o(\underline{k}+\underline{K}) + \sum_{\underline{K}} C^o(\underline{k},\underline{k}+\underline{K})\nabla_{\underline{R}}\Phi\Big|_{\underline{R}^o} + \sum_{\underline{K}} \nabla_{\underline{R}}C\Big|_{\underline{R}^o}\Phi^o(\underline{k}+\underline{K}) + \sum_{\underline{k}'\neq\underline{k}+\underline{K}} \nabla_{\underline{R}}C\Big|_{\underline{R}^o}\Phi^o(\underline{k}')$$

$$\simeq \Psi^o_{\underline{k}} + \sum_{\text{all } \underline{k}'} \nabla_{\underline{R}}C\Big|_{\underline{R}^o}\Phi^o(\underline{k}') + \sum_{\underline{K}} C^o(\underline{k},\underline{k}+\underline{K})\nabla_{\underline{R}}\Phi\Big|_{\underline{R}^o} \qquad (2\text{-}49)$$

The second term of (2-49) represents scattering into an available equilibrium eigenstate, since the sum is over all possible $\underline{k}'$ states and reciprocal lattice vectors $\underline{K}$. "Available" is emphasized because all scattering is considered from the ground state configuration, and the lowest energy eigenstates are filled to the Fermi level and are NOT available as final states into which scattering occurs. Rewriting the second term to emphasize this fact

$$\begin{aligned} S_{\underline{k}} &= \sum_{\text{all } \underline{k}'} \nabla_{\underline{R}} C \Big|_{\underline{R}^o} \Phi^o(\underline{k}') \\ &= \sum_{\underline{k}'} A(\underline{k}';\underline{k}) \Psi^o_{\underline{k}'} \end{aligned} \tag{2-50}$$

where the sum $\underline{k}'$ over the scattered states is now restricted to the excited or conduction band eigenstates.

The third term of (2-49) is seen [through the unperturbed coefficients $C^o(\underline{k},\underline{k}+\underline{K})$] to allow the unperturbed APW basis function to follow the motion of the nuclei and the rest (those not in the j^{th} band and $\underline{k}^{th}$ vector eigenstate) of the electrons. This is also pointed out by Kenney[34] in a different context. For convenience, this term will be rewritten as

$$B_{\underline{k}} = \sum_{\underline{K}} C^o(\underline{k},\underline{k}+\underline{K}) \nabla_{\underline{R}} \Phi \Big|_{\underline{R}^o} \tag{2-51}$$

Comparing (2-44) and (2-49) shows that

$$\frac{M(\underline{k}';\underline{k})}{E^o_{\underline{k}} - E^o_{\underline{k}'}} = \langle \Psi^o_{\underline{k}'} | B_{\underline{k}} \rangle + \langle \Psi^o_{\underline{k}'} | S_{\underline{k}} \rangle \tag{2-52}$$

The electronic Schrödinger equation for the perturbed situation may be taken from (2-3) as

$$H_e \Psi_{\underline{k}} = E_{\underline{k}} \Psi_{\underline{k}} \tag{2-53}$$

with $V_e(\underline{r})$ and $V_{ne}(\underline{r},\underline{R})$ the sum of displaced muffin-tin potentials

$$V_{ne}(\underline{r},\underline{R}) + V_e(\underline{r}) = \sum_j V_{MT}(\underline{r}-\underline{R}_j) \qquad (2\text{-}54)$$

and j labeling the nuclei and their respective muffin-tins.

Expanding (2-53) and (2-54) about the $\underline{R}_j^o$ equilibrium positions to terms linear in the lattice displacements $(\delta\underline{R}_j)$, one finds

$$H_e^o(\underline{R}^o)[S_{\underline{k}} + B_{\underline{k}}] + \delta V\Psi^o_{\underline{k}} = E^o_{\underline{k}}(S_{\underline{k}} + B_{\underline{k}}) \qquad (2\text{-}55)$$

with $H_e^o(\underline{R}^o)\Psi^o_{\underline{k}} = E^o_{\underline{k}}\Psi^o_{\underline{k}}$ and $\delta V = \sum_j \delta\underline{R}_j \cdot \frac{\partial V_{MT}}{\partial \underline{R}_j}\Big|_{\underline{R}_j^o}$.

(2-50) and (2-52) may be used to obtain

$$\frac{M(\underline{k}';\underline{k})}{E^o_{\underline{k}} - E^o_{\underline{k}'}} = A(\underline{k}';\underline{k}) + \langle\Psi^o_{\underline{k}'}|B_{\underline{k}}\rangle \qquad (2\text{-}56)$$

Solving for $A(\underline{k}';\underline{k})$ by using (2-55) gives

$$(E^o_{\underline{k}'} - E^o_{\underline{k}})A(\underline{k}';\underline{k}) = (E^o_{\underline{k}} - E^o_{\underline{k}'})\langle\Psi^o_{\underline{k}'}|B_{\underline{k}}\rangle - \langle\Psi^o_{\underline{k}'}|\delta V|\Psi^o_{\underline{k}}\rangle \qquad (2\text{-}57)$$

With the use of (2-57) and (2-56), the final expression for the EPME becomes

$$M(\underline{k}';\underline{k}) = \langle\Psi^o_{\underline{k}'}|\sum_j \delta\underline{R}_j \cdot \frac{\partial V_{MT}}{\partial \underline{R}_j}\Big|_{\underline{R}_j^o}|\Psi^o_{\underline{k}}\rangle \qquad (2\text{-}58)$$

In Figure 2-3, the "rigid ion" assumption is illustrated, showing that the potential at any point within the jth muffin-tin is the same, with respect to the center of that muffin-tin, regardless of the displacement

$$\underline{r}_j = \underline{r}_j^o - \underline{R}_j^o = \underline{r} - \underline{R}_j \qquad (2\text{-}59)$$

with $\delta\underline{R}_j = \underline{R}_j - \underline{R}_j^o$ and that as a consequence the potential gradient

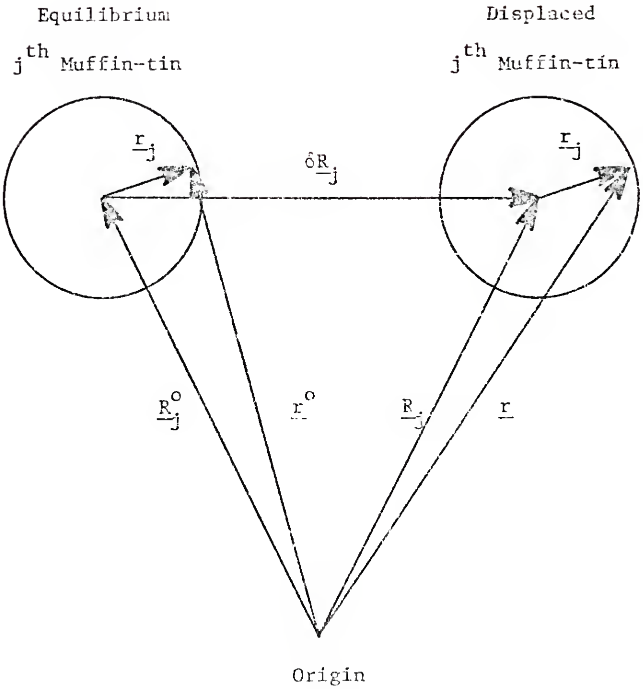

Figure 2-3. Demonstration of rigid ion approximation for muffin-tin displacement. This figure shows that the potential with respect to the muffin-tin center is the same regardless of displacement.

of (2-58) may be written as

$$\left.\frac{\partial V_{MT}(\underline{r}_j)}{\partial \underline{R}_j}\right|_{\underline{R}_j^o} = -\left.\frac{\partial V_{MT}(\underline{r}_j)}{\partial \underline{r}}\right|_{\underline{R}_j^o} = -\frac{\partial V_{MT}(\underline{r}_j)}{\partial \underline{r}^o} \qquad (2\text{-}60)$$

Since the MT potential is spherically symmetric within the sphere radius and constant outside the sphere radius, (2-60) becomes

$$\nabla V_{MT}(\underline{r}) = \hat{e}_r \frac{dV}{dr} \qquad \text{for } r<R_s$$

$$= 0 \qquad \text{for } r>R_s \qquad (2\text{-}61)$$

where $\hat{e}_r$ is the unit radial vector.

In section 2-4, the nuclear displacements ($\delta\underline{R}_j$) were expanded in normal mode coordinates for use in the assumed EPME expression (2-31). Comparison between (2-31) and (2-58) shows that the APW form of the EPME may be written

$$M(\underline{k}';\underline{k}) = (MN2\omega^o_{\underline{q}\lambda})^{-1/2} \int_{j^{th}\ \text{unit cell}} \psi^o_{\underline{k}'}(\underline{r})\underline{\varepsilon}_{\underline{q}\lambda}\cdot\nabla_{\underline{R}_j} V_{MT}\psi^o_{\underline{k}}(\underline{r})\, d\underline{r} \qquad (2\text{-}62)$$

where $\underline{\varepsilon}_{\underline{q}\lambda}$ is the eigenvector and $\omega^o_{\underline{q}\lambda}$ is the energy or frequency of the $\underline{q}^{th}$ phonon of λ polarization, M on the RHS is the nuclear mass, and N is the number of nuclei or unit cells (for a Bravais lattice). Using (2-61) and (2-60), the final expression for the EPME becomes

$$M(\underline{k}';\underline{k}) = -(MN2\omega^o_{\underline{q}\lambda})^{-1/2} \int_{j^{th}\ \text{sphere}} \psi^o_{\underline{k}'}(\underline{r})\underline{\varepsilon}_{\underline{q}\lambda}\cdot\hat{e}_r \frac{dV_{MT}}{dr}\psi^o_{\underline{k}}(\underline{r})\, d\underline{r} \qquad (2\text{-}63)$$

where the selection rule of section 2-4 (2-33) or Appendix II (A2-3) must be satisfied. Appendix II shows that this selection rule allows only certain transitions between the representations of the electron wave vectors and the polarizations of the phonon wave vector. In Appendix III, explicit formulae are derived for the SAPW basis function (2-22) form of (2-63).

CHAPTER III

RESULTS OF CALCULATION

3-1. APW Energy Band Calculation of Argon and Neon

The Xα energy bands and wave functions in argon and neon have been calculated for the two highest occupied valence bands and the lowest unoccupied conduction band. For neon, this would correspond to the "2s-like" "2p-like", and "3s-like" bands; and for argon, the "3s-like", "3p-like", and "4s-like" bands. The other lower lying core bands were treated in the usual fashion as states of the crystalline potential having atomic-like character; thus they correspond to flat (*i.e.* *k*-independent) bands.

As is expected for an insulator, the valence bands of argon and neon are completely filled with a definite energy gap between the highest valence band and the bottom of the conduction band. By construction, the bands also exhibit the features characteristic of fcc structures.[35]

All band calculations were done at nineteen symmetry inequivalent *k* points in the irreducible wedge (see Figure A2-1 and Appendix II). This corresponds to 256 possible wave vectors or a 4x4x4 periodic macro-cell (64 unit cells with 4 atoms per unit cell for the fcc structure). The angular momentum sums were evaluated through $\ell=10$ and the maximum square magnitude used for a reciprocal vector was $80\pi^2/a^2$. Iteration-to-iteration convergence on the total energy was typically at least 10^{-6} Ryd. and usually better. As a result of this energy convergence, the pressure, virial ratio, and potential also were well converged which ensured numerically the best possible eigenvalues and eigenfunctions.

Relevant results of the neon calculations are given in Table 3-1. In that Table, "X-Alpha Equilibrium" refers to the static lattice constant determined to correspond to the lowest crystalline total energy. "Experimental Equilibrium" means the calculation done at the experimental constant.

Neon at the calculated equilibrium lattice constant (7.7 a.u.) is seen to be overbound (in comparison with experiment) by a factor of two. This overbinding is also evident in the valence and conduction bands. The valence band widths are expanded by nearly a factor of two as compared with the other neon (8.4348 a.u.) calculation. The bottom of the excited "3p-like" conduction band extends into the excited "3s-like" conduction band; in all the other calculations (including argon), the lowest excited conduction bands are well separated. This extension would add in principle, another representation to the "s-like" representations of Table A2-1, which were used in the actual selection rules between the "p-like" valence (occupied) and the "s-like" conduction (unoccupied) bands. However, the additional contribution was not considered in the calculation of the phonon energy corrections and only the "s-like" representations of Table A2-1 were used in the calculations.

The argon results of Table 3-2 appear to be very good, particularly the calculated cohesive energy. However, the calculated band gap is only about sixty percent of the experimental value.

Since this work is not a comparative study of one-electron models, but an attempt to extend a particularly familiar example of such a model into a previously unexplored area, a discussion of the relative merits of the Xα calculations is not necessary. Rather, the best possible solutions of the Xα-model that can be obtained will be utilized, regardless of experimental comparison.

Table 3-1

Calculated and Observed Properties of Neon [a]

	Calculated		Observed
	X-Alpha Equilibrium	Experimental Equilibrium	Experimental Value [b]
Lattice Constant	7.7	8.4348	8.4323
Atomic Mass $_{10}Ne^{20}$	(3.644308×10^{4})	(3.644308×10^{4})	3.644308×10^{4}
Exchange Parameter-Alpha	2/3	2/3	-
Pressure (in kilobars)	-0.24	-4.59	0.0
Total Energy	-254.9852860	-254.9844249	-
Total Atomic Energy [c]	-254.9815919	-254.9815919	-
Cohesive Energy	-0.0036941	-0.002833	-0.0019186
Zero Point Energy	9.3644×10^{-4}	7.5127×10^{-4}	4.9082×10^{-4}
Lennard-Jones Parameters			
ε	4.29037×10^{-4}	3.29028×10^{-4}	2.2990×10^{-4}
σ	4.99436556	5.47097073	5.2695
Quantum Parameter [d]	5.128128×10^{-3}	5.572535×10^{-3}	8.3457×10^{-3}

[a] All quantities are in Rydberg atomic units except where noted

[b] See references 21 and 36

[c] See reference 24

[d] See Appendix I for definition

Table 3-2

Calculated and Observed Properties of Argon [a]

	Calculated		Observed
	X-Alpha Equilibrium	Experimental Equilibrium	Experimental Value [b]
Lattice Constant	9.66773	10.039	10.039
Atomic Mass $_{18}Ar^{40}$	(7.2845784×10^4)	(7.2845784×10^4)	7.2845784×10^4
Exchange Parameter-Alpha	0.72131	0.72131	-
Pressure (in kilobars)	-1.21	-3.99	0.0
Total Energy	-1053.603303	-1053.602791	-
Total Atomic Energy [c]	-1053.596648	-1053.596648	-
Cohesive Energy	-0.006655	-0.006143	-0.006479
Zero Point Energy	6.7300×10^{-4}	6.2250×10^{-4}	5.9600×10^{-4}
Lennard-Jones Parameters			
ε	7.72920×10^{-4}	7.13456×10^{-4}	7.55570×10^{-4}
σ	6.27067	6.51149	6.51149
Quantum Parameter [d]	9.03364×10^{-4}	9.07608×10^{-4}	8.57550×10^{-4}

[a] All quantities are in Rydberg atomic units except where noted

[b] See references 21 and 36

[c] See reference 23

[d] See Appendix I for definition

3-2. The SCH Phonon Spectra of Argon and Neon

As mentioned in section 2-1, SCH theory, instead of conventional harmonic theory, was used to calculate the phonon spectra of argon and neon because of zero point motion considerations. In addition, it was felt that SCH theory represents a conceptual improvement over quasi-harmonic theory for the calculation of unperturbed phonons.

All phonon calculations used an extremely fine reciprocal space mesh (large number of phonon wave vectors). Symmetry considerations allow the calculation to be done in the irreducible wedge of the first BZ (see Figure A2-1 and Appendix II). Thus, the six non-equivalent wave vectors used in the selection rules and their respective frequencies represent a small subset of the calculated frequencies.

Due to the three polarizations of the phonons and to degeneracies of the phonons among these polarizations, the set of six points corresponds to twelve energetically different phonons. These twelve phonons and their respective representations are listed as "Bare Phonons" in Table 3-3 for neon and Table 3-4 for argon.

The overbinding of neon in the Xα model is reflected in the "bare" phonon spectra. This is expected since the static solid cohesive energy is included in the Lennard-Jones pair potential description. The bare phonons for neon at 7.7 a.u. are a factor of two higher than the experimentally determined phonons. Though the 8.4348 a.u. calculation is less overbound, the "bare" phonon frequencies are still substantially different from the experimental frequencies.

The static lattice cohesive energy (given in Tables 3-1 and 3-2) and the average total energy per particle, determined in the dynamic lattice using SCH, have been used to calculate the zero point energy. The resul-

Table 3-3

Comparison of the Calculated and Experimental Neon Phonons

Representation[b]	Calculation				Experiment[a]
	a=7.7 a.u.		a=8.4348 a.u.		a=8.4395 a.u.
	Bare Phonons	Perturbed Phonons	Bare Phonons	Perturbed Phonons	
Γ_{15}	0.0[c]	0.0	0.0	0.0	0.0
Δ_1	2.327	2.709	1.873	2.194	1.120
Δ_5	1.619	2.063	1.301	1.675	0.805
X_4'	3.375	3.560	2.715	2.873	1.726
X_5'	2.285	2.532	1.837	2.045	1.139
Σ_1	2.891	3.161	2.326	2.559	1.395
Σ_3	2.343	2.544	1.884	2.060	1.129
Σ_4	1.512	2.001	1.216	1.618	0.745
L_2'	3.389	3.619	2.726	2.927	1.603
L_3'	1.513	1.974	1.216	1.597	0.752
W_2'	2.267	2.617	1.823	2.110	–
W_3	2.886	3.102	2.321	2.505	–

[a] Experimental results are from reference 37 and are at T = 6.5°K

[b] Symmetry labels of phonons are those of reference 29

[c] Frequency units are 10^{12} Hz (THz)

Table 3-4

Comparison of the Calculated and Experimental Argon Phonons

	Calculation				Experiment[a]
	a=9.66773 a.u.		a=10.039 a.u.		a=10.040 a.u.
Representation[b]	Bare Phonons	Perturbed Phonons	Bare Phonons	Perturbed Phonons	
Γ_{15}	0.0[c]	0.0	0.0	0.0	0.0
Δ_1	1.599	1.848	1.480	1.723	1.342
Δ_5	1.124	1.399	1.040	1.288	0.958
X_4'	2.333	2.434	2.159	2.282	1.909
X_5'	1.588	1.762	1.469	1.634	1.363
Σ_1	1.994	2.171	1.845	2.021	1.716
Σ_3	1.624	1.745	1.503	1.627	1.356
Σ_4	1.054	1.428	0.976	1.284	0.906
L_2'	2.337	2.486	2.163	2.309	1.915
L_3'	1.055	1.366	0.976	1.270	0.911
W_2'	1.573	1.814	1.456	1.677	–
W_3	1.999	2.143	1.849	1.989	–

[a] Experimental results are from reference 38 and are for $_{18}Ar^{36}$ at T=10°K. Phonons have been scaled by $(36/40)^{1/2}$.

[b] Symmetry labels of phonons are from reference 29

[c] Frequency units are 10^{12} Hz (THz)

ting values and the estimated true zero point energy are listed in Tables 3-1 and 3-2. The overbinding of neon is seen again to be reflected in this calculated zero point energy.

The argon phonons compare more favorably with experiment, due to the better agreement between the calculated and experimental static cohesive energy. The calculated zero point energy for argon also compares well with experiment.

3-3. The Perturbed Phonon Spectra of Argon and Neon

The calculation of the perturbed phonons is crude in the sense that a periodic macro-cell of eight cubic unit cells (2x2x2) has been used for the calculation. The APW and SCH calculations were done with larger periodic macro-cells to ensure the accurate representation of the solid based on the smaller macro-cell. This smaller macro-cell is equivalent to 32 atoms since the fcc crystal structure has four atoms per cubic unit cell. In the actual evaluation of the EPME expressions and selection rules, only six non-equivalent wave vectors of the electrons and phonons (corresponding to 32 possible wave vectors) were considered. As pointed out in Appendix II, these six wave vectors have associated with them twelve representations for the phonons and the "p-like" electrons, and six representations for the "s-like" electrons.

Since the "p-like" valence bands are full, the transition from any $\underline{k}$ state in the p band is only possible to any empty $\underline{k}'$ state in the conduction bands. In view of the energy difference denominator for the second order energy corrections (2-42), it was deemed sufficient to sum over all possible $\underline{k}'$ states in the lowest "s-like" conduction band.

As the ℓ sum limit of the APW calculation was 10, the EPME expressions of Appendix III could only be summed through $\ell=9$ because of the presence of terms dependent on $(\ell+1)$. The same square magnitude for the reciprocal lattice vectors was used as in the APW calculation.

The perturbed phonons for neon and argon are listed in Tables 3-3 and 3-4 respectively. Typically most bare phonons were perturbed from approximately ten to thirty percent. This is to be expected in view of the discussion (see also section 2-4) by Hedin and Lundqvist[30] of substantial corrections to the bare phonons given by the Fröhlich Hamiltonian. However, phonons of both neon and argon are corrected by about the same percentage so the method in general appears to be reasonable. That is, the phonon corrections do not appear to reflect the overbinding situation in neon.

The neon perturbed phonons are in both cases poor because the bare phonons reflect the overbinding. The argon results are substantially better, probably as a consequence of the good agreement between the calculated and experimental static cohesive energy. Though the good agreement for the argon cohesive energy may be fortuitous, the method of calculating the second order energy corrections would seem to give good results if the bare phonons are a reasonably decent representation of the dynamic lattice without the electron-phonon interaction.

CHAPTER IV

CONCLUSIONS

The purpose of this work has been to develop a feasible first principles (or nearly so) approach to the calculation of the effects of the electron-phonon interaction in an insulating solid. The problem was formulated in the APW-Xα formalism as a means of obtaining some computationally practical realization of the calculation. This utilization of the Xα model, in a way which had not been previously attempted, clearly constitutes a test of the method. Nevertheless, it was not the purpose of this work to weigh the merits of various density functional or local exchange schemes. Rather, the purpose was to see to what extent the features of a prototype density functional model, with all its admitted shortcomings, could be exploited for unconventional purposes.

The results and discussion in section 3-3 indicated that the method seemed to be a reasonable approach, even though a rather crude calculation was done. This is encouraging in view of the approximations made to achieve the calculation. Also it seems reasonable, based on the results of Chapter III, that better "bare" phonons and crystalline potentials would give much better agreement with experiment. The unrealistic nature (at least as compared with the results from potentials known to be reasonable) of the bare phonons used here can be traced, in part, to the assumed Lennard-Jones pair potential.[39] At best, such a pair potential is well known to be inadequate to describe a rare gas crystal. Moreover, we have already seen that the Xα model overbinds neon severely and argon slightly, so that the calculated equilibrium geometry is compressed with respect to the observed lattice. An improved functional form for the electronic Hamiltonian would be very desirable on these grounds alone. When one considers the problems with the Xα band gap in argon, and the consequent likelihood that the Xα static lattice conduction band states are of less than optimum quality, the value of an improved electronic Hamiltonian becomes even more obvious. In spite of these drawbacks, it remains a somewhat remarkable fact that a model as simple as Xα can be extended so far as to yield a respectable estimate of phonon dispersion in a rare gas crystal.

In the present APW realization of the formalism, however, it is not practical computationally to undertake more refined calculations. The problem is simply that of excessive computer time (see Appendix IV). This is a direct consequence of the energy-dependent APW basis, a problem met in other related work.[40] A change of basis functions, to say, a Gaussian type, (once the APW method has been used to calculate the eigenvalues and Bloch functions) would reduce substantially the computational labor of constructing a different basis set at each eigenvalue. The analogue for solids of Sambe's molecular work,[41] for instance, (a Gaussian basis Xα method) would be appropriate.

The results represent an attempt, within certain approximations and assumptions, at a first principles (or nearly so) calculation of microscopic lattice dynamics. A more rigorous approach would include the dielectric function, and not assume screening effects as this work has done. However, this would complicate the calculation by requiring the additional computation of the dielectric function and its inverse, a difficult task. Clearly, the use of the Lennard-Jones form for the unperturbed nuclear motion represents an intuitively plausible circumvention of these difficulties.

If the method can be refined and made computationally practical, it could, one might hope, be applied to calculations of other effects caused by the electron-phonon interaction. Based on this work, the calculation and method appear, in general, to be promising. This conclusion is probably the most important result of this work: the demonstration of the computational accessibility of the EPME given certain approximations. With the calculation now known to be at least possible, one may hope to achieve better quantitative understanding of electron-phonon effects in a solid by direct numerical investigation.

APPENDIX I

SELF-CONSISTENT HARMONIC APPROXIMATION AND LENNARD-JONES PAIR POTENTIALS

Since the unperturbed or "bare" phonons were calculated from computer codes written by T.R. Koehler, we shall follow the SCH treatment and notation developed by Koehler in a series of articles.[14,42,43] Following Koehler, we direct our attention to a one-dimensional single particle treatment to obtain the basic ideas and concepts of the SCH framework. This treatment is only intended to be representative.

Consider a particle with a total Hamiltonian H expressed in energy units of ε and in length units of σ and having a mass M,

$$H = T + V \tag{A1-1}$$

where $T = -1/2\ \Lambda^2\nabla^2$ and V is the potential energy. Λ^2 is a quantum parameter $(= \hbar^2/M\sigma^2\varepsilon)$, related to de Boer's parameter[44] by a factor of $(2\pi)^2$.

Taking the harmonic approximation to H (expanded about x=0) and writing it as h, we get

$$h = T + V^o + 1/2\ x^2\Phi \tag{A1-2}$$

where $V^o = V|_{x=0}$ and $\Phi = \nabla\nabla V|_{x=0}$. The quantum mechanical solution of the harmonic oscillator is well known and the normalized ground state eigenfunction is

$$|0\rangle = (G/\pi)^{1/4}\ \exp[-1/2\ x^2G] \tag{A1-3}$$

where $G^2 = \Phi/\Lambda^2$.

Taking the ground state expectation value of H yields

$$E^{o} = \langle 0|H|0\rangle = 1/4\ \Lambda^{2}G + \langle 0|V|0\rangle \qquad \text{(A1-4)}$$

where $\langle\Psi|\nabla\nabla|\Psi\rangle = 1/2\ \langle\Psi|\{\nabla\nabla \ln\Psi\}|\Psi\rangle$ has been used.

Minimizing E^{o} with respect to G and taking explicit account of the normalization gives

$$\frac{\partial E}{\partial G} = 0 = 1/4\ \Lambda^{2} - \frac{\langle 0|x^{2}V|0\rangle}{\langle 0|0\rangle} + \frac{\langle 0|x^{2}|0\rangle\langle 0|V|0\rangle}{\langle 0|0\rangle^{2}} \qquad \text{(A1-5)}$$

To evaluate (A1-5), some ground state matrix elements are needed. Consider

$$\nabla|0\rangle = -xG|0\rangle \qquad \text{(A1-6)}$$

Using (A1-6) to evaluate $\nabla((|0\rangle)^{2}V)$ yields the identity

$$(|0\rangle^{2}V)\Big|_{-\infty}^{+\infty} = -2\langle 0|xGV|0\rangle + \langle 0|\nabla V|0\rangle \qquad \text{(A1-7)}$$

However the LHS vanishes because the wave function is well behaved at plus or minus infinity; therefore we get

$$1/2\ G^{-1}\langle 0|\nabla V|0\rangle = \langle 0|xV|0\rangle \qquad \text{(A1-8)}$$

Operating on $((|0\rangle)^{2}V)$ with $\nabla\nabla$ and using (A1-7) and (A1-8) gives

$$\langle 0|x^{2}V|0\rangle = 1/2\ G^{-1}\langle 0|V|0\rangle + 1/4\ G^{-2}\langle 0|\nabla\nabla V|0\rangle \qquad \text{(A1-9)}$$

If we let V be unity, (A1-9) reduces to

$$\langle 0|x^{2}|0\rangle = 1/2\ G^{-1}\langle 0|0\rangle \qquad \text{(A1-10)}$$

Using the identities (A1-9) and (A1-10) on (A1-5) yields

$$0 = 1/4\ \Lambda^{2} - 1/4\ G^{-2}\frac{\langle 0|\nabla\nabla V|0\rangle}{\langle 0|0\rangle} \qquad \text{(A1-11)}$$

which is satisfied provided

$$\Lambda^2 G^2 = \langle 0|\nabla\nabla V|0\rangle = \Phi \qquad \text{(A1-12)}$$

Eqn. (A1-12) is the self-consistent requirement and shows the fundamental difference between ordinary classical harmonic theory and SCH lattice dynamics. The force constant is classical harmonic theory is the second derivative of the potential at equilibrium; the force constant in (A1-12) is a ground state average to be solved self-consistently through G. G is seen to be explicit on the LHS of (A1-12) and to be implicit on the RHS through $|0\rangle$. The extension of the above derivation to three dimensions and N particles of a crystalline solid is readily done (see Koehler[43]). The transformation of the problem to reciprocal space simplifies the actual numerical calculation, just as in ordinary lattice dynamics.

The potential corresponding to (A1-1) for the crystal problem is assumed most commonly to be a pairwise superposition of atomic potentials

$$V = 1/2 \sum_{i,j}{}' v(r_{ij}) \qquad \text{(A1-13)}$$

A fairly standard and widely used potential (especially for rare gas solids) is the Lennard-Jones (12-6) potential

$$v(r_{ij}) = 4\varepsilon[(\sigma/r_{ij})^{12} - (\sigma/r_{ij})^6] \qquad \text{(A1-14)}$$

This potential has a zero at $r_{ij} = \sigma$ and an energy minimum of $-\varepsilon$ at $r_{ij} = 2^{1/6}\,\sigma$.

Since we want to fit ε and σ to our APW results, we need the total energy expression and the volume derivative of the total energy expression at equilibrium volume. By choosing an N atom solid with our coordinate system origin centered on an atom, we may evaluate the total classical energy as

$$E = N/2 \sum_{i=1}^{N-1} v(r_i) \qquad \text{(A1-15)}$$

where r_i is the non-zero distance of the i^{th} atom from the origin.

The stable lattices for argon and neon are face-centered cubic (fcc) with the volume per primitive unit cell

$$U = a^3/4 \qquad \text{(A1-16)}$$

where a is the cubic lattice parameter. The j^{th} atom in the lattice is located by

$$\underline{r}_j = a/2 \; [\, m_{xj}\hat{e}_x + m_{yj}\hat{e}_y + m_{zj}\hat{e}_z \,] \qquad \text{(A1-17)}$$

with $|\underline{r}_j| = r_j = a/2 \; m_j$, $m_j = (m_{xj}^2 + m_{yj}^2 + m_{zj}^2)^{1/2}$, with m_{xj} , m_{yj} , m_{zj} a set of integers appropriate to the j^{th} atom.

Using (A1-16) and (A1-17) , the following relations are obtained

$$r_j^3 = 2\, U\, m_j^3 \qquad \text{(A1-18a)}$$

$$dr_j/dU = 2/3 \; m_j^3/r_j^2 \qquad \text{(A1-18b)}$$

Minimizing the total energy with respect to U

$$dE/dU = 0 = N/2 \;\; 2/3 \sum_j \; m_j^3/r_j^2 \; dv/dr_j \qquad \text{(A1-19)}$$

From (A1-14) we have

$$dv/dr_j = 4\varepsilon[-12\sigma^{12}/r_j^{13} + 6\sigma^6/r_j^7] \qquad \text{(A1-20)}$$

Combining (A1-16), (A1-18), and (A1-20) gives the following

$$\sigma/a = 2^{-7/6} \; [\, \sum_j m_j^{-6} \,/ \sum_j m_j^{-12}]^{1/6} \qquad \text{(A1-21)}$$

The lattice sums in (A1-21) have been evaluated for the fcc, bcc, sc, and hcp structures.[15,45,46] Equation (A1-21) shows that σ/a is independent of the lattice constant and is determined solely by the crystal structure.

The cohesive energy or energy per particle may be found using (A1-15) and (A1-17) and solving for ε

$$\varepsilon = \sum_j \frac{1/2\ (E/N)}{[(\sigma/(m_j a/2))^{12} - (\sigma/(m_j a/2))^{6}]} \qquad \text{(A1-22)}$$

These two equations, (A1-22) and (A1-21), together with the appropriate lattice sums, have been used to fit ε and σ for a representative pair potential that best describes the lattice as calculated by the APW program. The resulting pair potential is utilized as input by Koehler's SCH program and the "bare" or unperturbed phonons are calculated.

APPENDIX II

GROUP THEORETICAL EXPLANATION OF THE TRANSITION SELECTION RULES

This appendix is concerned with the specific use and description of the group theory employed throughout this problem, particularly in deriving the appropriate selection rules and in the labeling of the bands, phonon dispersion curves, Brillouin zone, and wave vectors. Also the group operations of all the non-equivalent wave vectors and of the unique vectors in their corresponding stars are given.

The entire APW calculation was done in the irreducible wedge of the first Brillouin zone (BZ) appropriate to the fcc crystal. The reduced zone is shown in Figure A2-1, together with the irreducible wedge and the two $\underline{k}$ space mesh grids that were used. The labeling convention of Bouckaert, Smoluchowski, and Wigner (BSW)[29] is used throughout this dissertation for the energy bands, phonon dispersion curves, and all wave vector labels (electrons and phonons). The list of the six non-equivalent reduced zone vectors that were used in deriving the selection rules is given in Table A2-1.

The derivation of the selection rules is based on the theory developed by Zak[47] of small representations of the groups of the various reduced wave vectors. The selection rule is calculated as the transition probability between a state of wave vector $\underline{k}$ to a state of wave vector $\underline{k}'$ by a perturbation or excitation of wave vector symmetry $\underline{q}$. The actual calculation is usually done in the following integral form

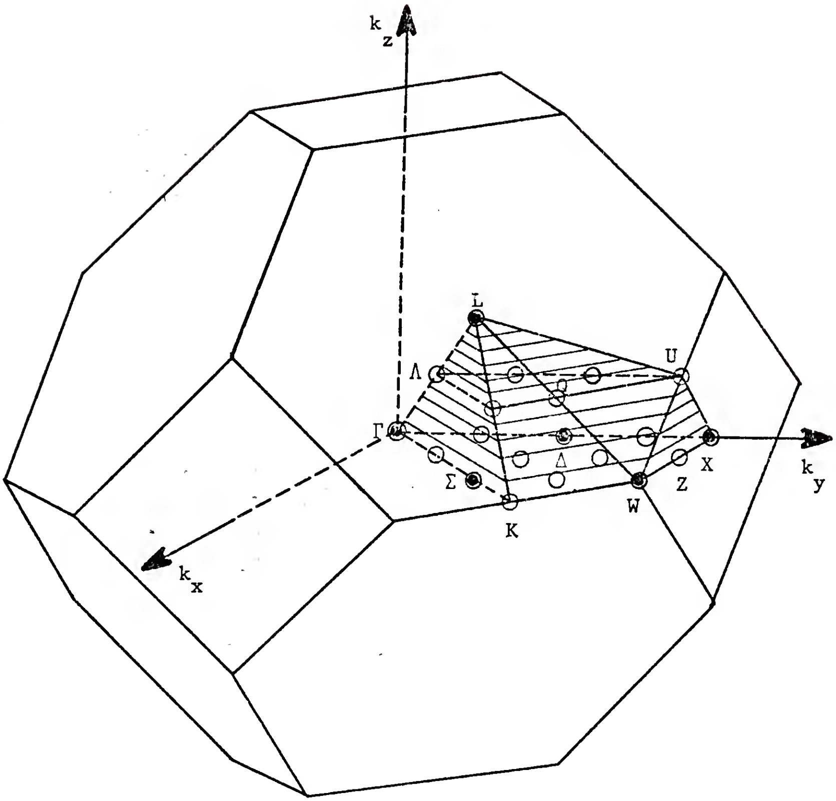

Figure A2-1. The first Brillouin zone for the fcc structure. The points labeled ● are those used in the 32 point grid (which corresponds to six non-equivalent points); while those points labeled ○ are the 256 point grid (which corresponds to nineteen non-equivalent points). The points K and U are equivalent and the wave vector axes are in π/a units, where a is the cubic lattice constant. The irreducible wedge (1/48th of the first zone) is shaded.

Table A2-1

Representations and Non-equivalent Reduced Wave Vectors

Reduced Wave Vector	Representations	
$\underline{k}$, $\underline{k}'$, $\underline{q}$ (units of π/a)	Phonon/p-like Valence	s-like Conduction
$\Gamma(0\ 0\ 0)$	Γ_{15}	Γ_1
$\Delta(0\ 1\ 0)$	$\Delta_1\ \ \Delta_5$	Δ_1
$X(0\ 2\ 0)$	$X_4'\ \ X_5'$	X_1
$\Sigma(1\ 1\ 0)$	$\Sigma_1\ \Sigma_3\ \Sigma_4$	Σ_1
$L(1\ 1\ 1)$	$L_2'\ L_3'$	L_1
$W(1\ 2\ 0)$	$W_2'\ W_3$	W_2'

$$\int \Psi^{*}_{\underline{k}'}(\underline{r}) V_{\underline{q}}(\underline{r}) \Psi_{\underline{k}}(\underline{r}) d\underline{r} \tag{A2-1}$$

where $\Psi_{\underline{k}}(\underline{r})$ is the initial state, $\Psi^{*}_{\underline{k}'}(\underline{r})$ is the final state, and $V_{\underline{q}}(\underline{r})$ is the perturbation connecting the two states. This integral vanishes unless $\underline{k} + \underline{q} = \underline{k}' + \underline{K}$ (where $\underline{K}$ is a reciprocal lattice vector), due to lattice symmetry.

Zak's treatment is done for general non-symorphic space groups and therefore can be somewhat simplified for the present work. We follow his notation and convention and let G_k, G_q, $G_{k'}$ stand for the groups of the vectors $\underline{k}$, $\underline{q}$, $\underline{k}'$ respectively. Letting g_c be the number of common group elements and G_c be the group of common elements among the three groups G_k, G_q, $G_{k'}$, one gets for the selection rule formula

$$1/g_c \sum_{R \in G_c} \xi_{ki}(R)\xi_{qj}(R)\xi_{k'l}(R) \tag{A2-2}$$

where $\xi_{ki}(R)$, $\xi_{qj}(R)$, $\xi_{k'l}(R)$ are the characters of the group element R in the i^{th}, j^{th}, l^{th} small representations of $\underline{k}$, $\underline{q}$, $\underline{k}'$ respectively. The above formula actually only tells whether a certain transition is allowed. However, by utilizing the wave vector selection rule inherent in (A2-1)

$$\underline{k} + \underline{q} = \underline{k}' + \underline{K} \tag{A2-3}$$

we can decompose the direct products between all small representations of $\underline{k}$ and $\underline{q}$ into all allowed small representations of $\underline{k}'$.

In this work, we are concerned with the face-centered cubic (fcc) crystal structure with one atom per primitive unit cell (i.e. O_h^5(Fm3m) space group in the Schoenflies and International Crystallography notation). The point group is O_h and in Table A2-2, we give the 48 group operations of this point group following the convention of von der Lage and Bethe.[48] Table A2-3 is the group multiplication table for the O_h point group.

Table A2-2

O_h Point Group Operations

Operation Number	Class	Matrix Representation	Vector Effect
1	E	1 0 0	x
		0 1 0	y
		0 0 1	z
2	C_4^2	-1 0 0	-x
		0-1 0	-y
		0 0 1	z
3	C_4^2	1 0 0	x
		0-1 0	-y
		0 0-1	-z
4	C_4^2	-1 0 0	-x
		0 1 0	y
		0 0-1	-z
5	C_4	0-1 0	-y
		1 0 0	x
		0 0 1	z
6	C_4	0 1 0	y
		-1 0 0	-x
		0 0 1	z
7	C_4	1 0 0	x
		0 0-1	-z
		0 1 0	y
8	C_4	1 0 0	x
		0 0 1	z
		0-1 0	-y
9	C_4	0 0 1	z
		0 1 0	y
		-1 0 0	-x
10	C_4	0 0-1	-z
		0 1 0	y
		1 0 0	x
11	C_2	0 1 0	y
		1 0 0	x
		0 0-1	-z

Table A2-2 continued

Operation Number	Class	Matrix Representation	Vector Effect
12	C_2	0 0 1 0-1 0 1 0 0	z -y x
13	C_2	-1 0 0 0 0 1 0 1 0	-x z y
14	C_2	0-1 0 -1 0 0 0 0-1	-y -x -z
15	C_2	0 0-1 0-1 0 -1 0 0	-z -y -x
16	C_2	-1 0 0 0 0-1 0-1 0	-x -z -y
17	C_3	0 0 1 1 0 0 0 1 0	z x y
18	C_3	0 1 0 0 0 1 1 0 0	y z x
19	C_3	0 0 1 -1 0 0 0-1 0	z -x -y
20	C_3	0-1 0 0 0-1 1 0 0	-y -z x
21	C_3	0 0-1 -1 0 0 0 1 0	-z -x y
22	C_3	0-1 0 0 0 1 -1 0 0	-y z -x
23	C_3	0 0-1 1 0 0 0-1 0	-z x -y

Table A2-2 continued

Operation Number	Class	Matrix Representation	Vector Effect
24 [a]	C_3	$\begin{matrix} 0 & 1 & 0 \\ 0 & 0 & -1 \\ -1 & 0 & 0 \end{matrix}$	y $-z$ $-x$

[a] The operations 25-48 are obtained by reversing the sign of the first 24 operations; *i.e.* they are the inversion operator (denoted by the class symbol J) times each of the first 24 operations. As an example, consider operation 4 times the inversion: the vector effect becomes (x -y z), the operation number becomes 28, and the class becomes JC_4^2.

Table A2-3

O_h Point Group Multiplication Table

Class		C_4^2			C_4						C_2						C_3								R	R^{-1}
	1	2	3	4	5	6	7	8	9	10	11	12	13	14	15	16	17	18	19	20	21	22	23	24	1	1
C_4^2	2	1	4	3	6	5	13	16	15	12	14	10	7	11	9	8	21	20	23	18	17	24	19	22	2	2
	3	4	1	2	14	11	8	7	12	15	6	9	16	5	10	13	19	24	17	22	23	20	21	18	3	3
	4	3	2	1	11	14	16	13	10	9	5	15	8	6	12	7	23	22	21	24	19	18	17	20	4	4
C_4	5	6	11	14	2	1	17	23	22	20	4	18	21	3	24	19	13	10	8	12	7	15	16	9	5	6
	6	5	14	11	1	2	21	19	24	18	3	20	17	4	22	23	7	12	16	10	13	9	8	15	6	5
	7	16	8	13	20	24	3	1	17	21	18	19	2	22	23	4	12	6	6	14	15	5	10	11	7	8
	8	13	7	16	22	18	1	3	19	23	24	17	4	20	21	2	9	11	12	5	10	14	15	6	8	7
	9	12	15	10	17	19	24	22	4	1	23	3	18	21	2	20	11	8	14	7	6	13	5	16	9	10
	10	15	12	9	23	21	20	18	1	4	17	2	22	19	3	24	5	13	6	16	14	8	11	7	10	9
C_2	11	14	5	6	3	4	23	17	18	24	1	22	19	2	20	21	8	9	13	15	16	12	7	10	11	11
	12	9	10	15	19	17	18	20	2	3	21	1	24	23	4	22	6	7	5	8	11	16	14	13	12	12
	13	8	16	7	18	22	4	2	21	17	20	23	1	24	19	3	10	5	15	11	9	6	12	14	13	13
	14	11	6	5	4	3	19	21	20	22	2	24	23	1	18	17	16	15	7	9	8	10	13	12	14	14
	15	10	9	12	21	23	22	24	3	2	19	4	20	17	1	18	14	16	11	13	5	7	6	8	15	15
	16	7	13	8	24	20	2	4	23	19	22	21	3	18	17	1	15	14	10	6	12	11	9	5	16	16
C_3	17	19	23	21	12	9	11	5	13	7	10	8	6	15	16	14	18	1	22	3	24	2	20	4	17	18
	18	22	20	24	8	13	10	12	6	11	7	5	9	16	14	15	1	17	2	23	4	19	3	21	18	17
	19	17	21	24	9	12	6	14	16	8	15	7	11	10	13	5	24	3	20	1	18	4	22	2	19	20
	20	24	18	22	16	7	12	10	5	14	13	6	15	8	11	9	2	21	1	19	3	23	4	17	20	19
	21	23	19	17	10	15	14	6	7	13	12	16	5	9	8	11	20	2	24	4	22	1	18	3	21	22
	22	18	24	20	13	8	9	15	14	5	16	11	10	7	6	12	4	23	3	17	1	21	2	19	22	21
	23	21	17	19	15	10	5	11	8	16	9	13	14	12	7	6	22	4	18	2	20	3	24	1	23	24
	24	20	22	18	7	16	15	9	11	6	8	14	12	13	5	10	3	19	4	21	2	17	1	23	24	23

$R_i R_j = R_k$ $k = 1$ to 24

$i,j = 1$ to 24 or $i,j = 25$ to 48

$R_{i+24} R_j = R_i R_{j+24} = R_{k+24}$

$i,j = 1$ to 24; $k = 1$ to 24

Only the filled p-like valence and the unfilled s-like conduction bands have been considered and allowed to interact. The p-like representations (associated with the vector $\underline{k}$), the s-like representations (associated with the vector $\underline{k}'$), and the representations associated with the phonon wave vector $\underline{q}$ are listed in Table A2-1. All wave vectors are in the reduced zone scheme and are in units of π/a, where a is the lattice constant.

In Table A2-4, are listed the group operations belonging to each of the 32 equivalent BZ points used throughout this work. This table and the character tables of the small representations of the wave vectors[29] will be used in the illustrative example that will follow.

As an example of the selection rule calculation consider an interaction involving the vectors $\underline{k}$ = (0 1 0) and $\underline{q}$ = (1 1 0), and the $\underline{k}$ representation Δ_1 and the $\underline{q}$ representation Σ_1. By using (A2-3), all possible allowed $\underline{k}'$ vectors are seen to be $\underline{k}'$ = (0 1 0), (1 1 1), and (1 2 0). Therefore one must use the selection rule formula on all the $\underline{k}'$ representations of Δ (0 1 0), L (1 1 1), and W (1 2 0).

Considering first only the Δ representations of $\underline{k}'$, Table A2-4 shows that the groups of operations associated with $\underline{q}$ = (1 1 0) and $\underline{k}$ = (-1 0 0) have only two group elements in common: the identity element in class E and an improper rotation element in class JC_4^2. Therefore the selection rule (A2-2) reduces to

$$1/2\ [\xi_{\Delta_1}(E)\xi_{\Sigma_1}(E)\xi_{\Delta i}(E) + \xi_{\Delta_1}(JC_4^2)\xi_{\Sigma_1}(JC_4^2)\xi_{\Delta i}(JC_4^2)] \qquad \text{(A2-4)}$$

The character tables in the BSW article[29] are used to reduce (A2-4) to

$$1/2\ [\xi_{\Delta i}(E) + \xi_{\Delta i}(JC_4^2)] \qquad \text{(A2-5)}$$

which when evaluated over all Δi representations shows that only the Δ_1,

Table A2-4

Group Operations of the Thirty-two Equivalent First BZ Points

Symmetry Point	Star Member (π/a units)	Group Operations
Γ	(0 0 0)	All 48 Operations
Δ	(1 0 0)	1 3 7 8 26 28 37 40
	(0 1 0)	1 4 9 10 26 27 36 39
	(0 0 1)	1 2 5 6 27 28 35 38
	(-1 0 0)	1 3 7 8 26 28 37 40
	(0 -1 0)	1 4 9 10 26 27 36 39
	(0 0 -1)	1 2 5 6 27 28 35 38
X	(2 0 0)	1 2 3 4 7 8 13 16 25 26 27 28 31 32 37 40
	(0 2 0)	1 2 3 4 9 10 12 15 25 26 27 28 33 34 36 39
	(0 0 2)	1 2 3 4 5 6 11 14 25 26 27 28 29 30 35 38
Σ	(1 1 0)	1 11 26 38
	(1 -1 0)	1 14 26 35
	(-1 1 0)	1 14 26 35
	(-1 -1 0)	1 11 26 38
	(1 0 1)	1 12 28 39
	(1 0 -1)	1 15 28 36
	(-1 0 1)	1 15 28 36
	(-1 0 -1)	1 12 28 39
	(0 1 1)	1 13 27 40
	(0 1 -1)	1 16 27 37
	(0 -1 1)	1 16 27 37
	(0 -1 -1)	1 13 27 40

Table A2-4 continued

Symmetry Point	Star Member (π/a units)	Group Operations
L	(1 1 1)	1 14 15 16 17 18 25 38 39 40 41 42
	(-1 1 1)	1 11 12 16 21 22 25 35 36 40 45 46
	(1 -1 1)	1 11 13 15 19 20 25 35 37 39 43 44
	(-1 -1 1)	1 12 13 14 23 24 25 36 37 38 47 48
W	(1 2 0)	1 3 13 16 26 28 31 32
	(2 1 0)	1 4 12 15 26 27 33 34
	(0 1 2)	1 4 12 15 26 27 33 34
	(0 2 1)	1 2 11 14 27 28 29 30
	(1 0 2)	1 3 13 16 26 28 31 32
	(2 0 1)	1 2 11 14 27 28 29 30

Δ_2, and Δ_5 representations contribute.

Applying these same techniques to the other two cases (the L (1 1 1) point and W (1 2 0) point), gives the following decomposition between the Δ_1 and Σ_1 representations

$$\Delta_1 \boxtimes \Sigma_1 = \Delta_1 \oplus \Delta_2 \oplus \Delta_5 \oplus L_1 \oplus L_2' \oplus L_3 \oplus L_3' \oplus W_1 \oplus W_2' \oplus W_3 \qquad \text{(A2-6)}$$

where $\boxtimes$ denotes direct product and $\oplus$ denotes direct sum of the representations.[49] As a check on the decomposition, the product of the star number (48 divided by the order of the group) times the dimensionality of each representation of the LHS of (A2-6) must be equal to the sum of the star number times the dimensionality of each representation on the RHS. Using (A2-6) as an example, we see that the LHS is equal to 72 [Δ_1 dim. = 1, star = (48/8) = 6; Σ_1 dim. = 1. star = (48/4) = 12] and the RHS is equal to 72 [Δ_1 dim. = 1, star = 6; Δ_2 dim. = 1, star = 6; Δ_5 dim. = 2, star = 6; L_1 dim. = 1, star = 4; L_2' dim. = 1, star = 4; L_3 dim. = 2, star = 4; L_3' dim. = 2, star = 4; W_1 dim. = 1, star = 6; W_2' dim. = 1, star = 6; W_3 dim. = 2, star = 6]. The direct product is also seen to be symmetric, i.e. $\Delta_1 \boxtimes \Sigma_1 = \Sigma_1 \boxtimes \Delta_1$.

In the actual calculation , only the representations that are in the s-like excited conduction band are used. From (A2-6) and Table A2-1, the only representations that contribute in our example are seen to be Δ_1, L_1, and W_2' . A list of all possible valence band to conduction band excitations for each $\underline{q}$ (phonon wave vector) representation has been constructed and is given in Table A2-5.

The electron-phonon matrix element (EPME) calculation has been simplified through the use of group theory. Specifically the EPME is first calculated for a fixed star member of the $\underline{k}'$ vector and all possible star

Table A2-5

Selection Rules between Valence p-like Band and Conduction s-like Band

$\underline{k}$ Representation		$\underline{q}$ Representation		$\underline{k}'$ Representation
Γ_{15}	$\otimes$	Γ_{15}	=	Γ_1
Δ_1	$\otimes$	Γ_{15}	=	Δ_1
Δ_5	$\otimes$	Γ_{15}	=	Δ_1
X_4'	$\otimes$	Γ_{15}	=	X_1
X_5'	$\otimes$	Γ_{15}	=	X_1
Σ_1	$\otimes$	Γ_{15}	=	No Contribution
Σ_3	$\otimes$	Γ_{15}	=	$2\Sigma_1$
Σ_4	$\otimes$	Γ_{15}	=	No Contribution
L_2'	$\otimes$	Γ_{15}	=	L_1
L_3'	$\otimes$	Γ_{15}	=	L_1
W_2'	$\otimes$	Γ_{15}	=	No Contribution
W_3	$\otimes$	Γ_{15}	=	W_2'
Γ_{15}	$\otimes$	Δ_1	=	Δ_1
Δ_1	$\otimes$	Δ_1	=	$X_1 \oplus \Sigma_1 \oplus \Gamma_1$
Δ_5	$\otimes$	Δ_1	=	Σ_1
X_4'	$\otimes$	Δ_1	=	Δ_1
X_5'	$\otimes$	Δ_1	=	W_2'
Σ_1	$\otimes$	Δ_1	=	$\Delta_1 \oplus L_1 \oplus W_2'$
Σ_3	$\otimes$	Δ_1	=	L_1
Σ_4	$\otimes$	Δ_1	=	$\Delta_1 \oplus W_2'$
L_2'	$\otimes$	Δ_1	=	Σ_1
L_3'	$\otimes$	Δ_1	=	Σ_1
W_2'	$\otimes$	Δ_1	=	$X_1 \oplus \Sigma_1$
W_3	$\otimes$	Δ_1	=	Σ_1

Table A2-5 continued

k Representation		q Representation		k' Representation
Γ_{15}	$\otimes$	Δ_5	=	Δ_1
Δ_1	$\otimes$	Δ_5	=	Σ_1
Δ_5	$\otimes$	Δ_5	=	$\Gamma_1 \oplus X_1 \oplus 2\Sigma_1$
X_4'	$\otimes$	Δ_5	=	W_2'
X_5'	$\otimes$	Δ_5	=	$\Delta_1 \oplus W_2'$
Σ_1	$\otimes$	Δ_5	=	$\Delta_1 \oplus L_1 \oplus W_2'$
Σ_3	$\otimes$	Δ_5	=	$\Delta_1 \oplus L_1 \oplus W_2'$
Σ_4	$\otimes$	Δ_5	=	$\Delta_1 \oplus L_1 \oplus W_2'$
L_2'	$\otimes$	Δ_5	=	Σ_1
L_3'	$\otimes$	Δ_5	=	$2\Sigma_1$
W_2'	$\otimes$	Δ_5	=	Σ_1
W_3	$\otimes$	Δ_5	=	$X_1 \oplus 2\Sigma_1$
Γ_{15}	$\otimes$	X_4'	=	X_1
Δ_1	$\otimes$	X_4'	=	Δ_1
Δ_5	$\otimes$	X_4'	=	W_2'
X_4'	$\otimes$	X_4'	=	$\Gamma_1 \oplus X_1$
X_5'	$\otimes$	X_4'	=	No Contribution
Σ_1	$\otimes$	X_4'	=	Σ_1
Σ_3	$\otimes$	X_4'	=	Σ_1
Σ_4	$\otimes$	X_4'	=	Σ_1
L_2'	$\otimes$	X_4'	=	L_1
L_3'	$\otimes$	X_4'	=	L_1
W_2'	$\otimes$	X_4'	=	No Contribution
W_3	$\otimes$	X_4'	=	Δ_1

Table A2-5 continued

$\underline{k}$ Representation		$\underline{q}$ Representation		$\underline{k}'$ Representation
Γ_{15}	$\otimes$	X_5'	=	X_1
Δ_1	$\otimes$	X_5'	=	W_2'
Δ_5	$\otimes$	X_5'	=	$\Delta_1 \oplus W_2'$
X_4'	$\otimes$	X_5'	=	No Contribution
X_5'	$\otimes$	X_5'	=	$\Gamma_1 \oplus 2X_1$
Σ_1	$\otimes$	X_5'	=	Σ_1
Σ_3	$\otimes$	X_5'	=	$2\Sigma_1$
Σ_4	$\otimes$	X_5'	=	Σ_1
L_2'	$\otimes$	X_5'	=	L_1
L_3'	$\otimes$	X_5'	=	$2L_1$
W_2'	$\otimes$	X_5'	=	No Contribution
W_3	$\otimes$	X_5'	=	$\Delta_1 \oplus W_2'$
Γ_{15}	$\otimes$	Σ_1	=	No Contribution
Δ_1	$\otimes$	Σ_1	=	$\Delta_1 \oplus L_1 \oplus W_2'$
Δ_5	$\otimes$	Σ_1	=	$\Delta_1 \oplus L_1 \oplus W_2'$
X_4'	$\otimes$	Σ_1	=	Σ_1
X_5'	$\otimes$	Σ_1	=	Σ_1
Σ_1	$\otimes$	Σ_1	=	$\Gamma_1 \oplus X_1 \oplus \Sigma_1$
Σ_3	$\otimes$	Σ_1	=	Σ_1
Σ_4	$\otimes$	Σ_1	=	Σ_1
L_2'	$\otimes$	Σ_1	=	$\Delta_1 \oplus W_2'$
L_3'	$\otimes$	Σ_1	=	$\Delta_1 \oplus W_2'$
W_2'	$\otimes$	Σ_1	=	$\Delta_1 \oplus W_2'$
W_3	$\otimes$	Σ_1	=	$\Delta_1 \oplus L_1 \oplus W_2'$

Table A2-5 continued

$\underline{k}$ Representation		$\underline{q}$ Representation		$\underline{k}'$ Representation
Γ_{15}	$\otimes$	Σ_3	=	$2\Sigma_1$
Δ_1	$\otimes$	Σ_3	=	L_1
Δ_5	$\otimes$	Σ_3	=	$\Delta_1 \oplus L_1 \oplus W_2'$
X_4'	$\otimes$	Σ_3	=	Σ_1
X_5'	$\otimes$	Σ_3	=	$2\Sigma_1$
Σ_1	$\otimes$	Σ_3	=	Σ_1
Σ_3	$\otimes$	Σ_3	=	$\Gamma_1 \oplus X_1 \oplus \Sigma_1$
Σ_4	$\otimes$	Σ_3	=	Σ_1
L_2'	$\otimes$	Σ_3	=	Δ_1
L_3'	$\otimes$	Σ_3	=	$\Delta_1 \oplus W_2'$
W_2'	$\otimes$	Σ_3	=	L_1
W_3	$\otimes$	Σ_3	=	$\Delta_1 \oplus L_1 \oplus W_2'$
Γ_{15}	$\otimes$	Σ_4	=	No Contribution
Δ_1	$\otimes$	Σ_4	=	$\Delta_1 \oplus W_2'$
Δ_5	$\otimes$	Σ_4	=	$\Delta_1 \oplus L_1 \oplus W_2'$
X_4'	$\otimes$	Σ_4	=	Σ_1
X_5'	$\otimes$	Σ_4	=	Σ_1
Σ_1	$\otimes$	Σ_4	=	Σ_1
Σ_3	$\otimes$	Σ_4	=	Σ_1
Σ_4	$\otimes$	Σ_4	=	$\Gamma_1 \oplus X_1 \oplus \Sigma_1$
L_2'	$\otimes$	Σ_4	=	No Contribution
L_3'	$\otimes$	Σ_4	=	$\Delta_1 \oplus W_2'$
W_2'	$\otimes$	Σ_4	=	$\Delta_1 \oplus L_1 \oplus W_2'$
W_3	$\otimes$	Σ_4	=	$\Delta_1 \oplus L_1 \oplus W_2'$

Table A2-5 continued

k Representation		q Representation		k' Representation
Γ_{15}	$\otimes$	L_2'	=	L_1
Δ_1	$\otimes$	L_2'	=	Σ_1
Δ_5	$\otimes$	L_2'	=	Σ_1
X_4'	$\otimes$	L_2'	=	L_1
X_5'	$\otimes$	L_2'	=	L_1
Σ_1	$\otimes$	L_2'	=	$\Delta_1 \oplus W_2'$
Σ_3	$\otimes$	L_2'	=	Δ_1
Σ_4	$\otimes$	L_2'	=	No Contribution
L_2'	$\otimes$	L_2'	=	$\Gamma_1 \oplus X_1$
L_3'	$\otimes$	L_2'	=	X_1
W_2'	$\otimes$	L_2'	=	Σ_1
W_3	$\otimes$	L_2'	=	Σ_1
Γ_{15}	$\otimes$	L_3'	=	L_1
Δ_1	$\otimes$	L_3'	=	Σ_1
Δ_5	$\otimes$	L_3'	=	$2\Sigma_1$
X_4'	$\otimes$	L_3'	=	L_1
X_5'	$\otimes$	L_3'	=	$2L_1$
Σ_1	$\otimes$	L_3'	=	$\Delta_1 \oplus W_2'$
Σ_3	$\otimes$	L_3'	=	$\Delta_1 \oplus W_2'$
Σ_4	$\otimes$	L_3'	=	$\Delta_1 \oplus W_2'$
L_2'	$\otimes$	L_3'	=	No Contribution
L_3'	$\otimes$	L_3'	=	$\Gamma_1 \oplus 2X_1$
W_2'	$\otimes$	L_3'	=	Σ_1
W_3	$\otimes$	L_3'	=	Σ_1

Table A2-5 continued

k Representation		q Representation		k' Representation
Γ_{15}	$\otimes$	W_2'	=	No Contribution
Δ_1	$\otimes$	W_2'	=	$X_1 \oplus \Sigma_1$
Δ_5	$\otimes$	W_2'	=	Σ_1
X_4'	$\otimes$	W_2'	=	No Contribution
X_5'	$\otimes$	W_2'	=	No Contribution
Σ_1	$\otimes$	W_2'	=	$\Delta_1 \oplus W_2'$
Σ_3	$\otimes$	W_2'	=	L_1
Σ_4	$\otimes$	W_2'	=	$\Delta_1 \oplus L_1 \oplus W_2'$
L_2'	$\otimes$	W_2'	=	Σ_1
L_3'	$\otimes$	W_2'	=	Σ_1
W_2'	$\otimes$	W_2'	=	$\Gamma_1 \oplus X_1 \oplus \Sigma_1$
W_3	$\otimes$	W_2'	=	Σ_1
Γ_{15}	$\otimes$	W_3	=	W_2'
Δ_1	$\otimes$	W_3	=	Σ_1
Δ_5	$\otimes$	W_3	=	$2X_1 \oplus 2\Sigma_1$
X_4'	$\otimes$	W_3	=	Δ_1
X_5'	$\otimes$	W_3	=	$\Delta_1 \oplus W_2'$
Σ_1	$\otimes$	W_3	=	$\Delta_1 \oplus L_1 \oplus W_2'$
Σ_3	$\otimes$	W_3	=	$\Delta_1 \oplus L_1 \oplus W_2'$
Σ_4	$\otimes$	W_3	=	$\Delta_1 \oplus L_1 \oplus W_2'$
L_2'	$\otimes$	W_3	=	Σ_1
L_3'	$\otimes$	W_3	=	$2\Sigma_1$
W_2'	$\otimes$	W_3	=	Σ_1
W_3	$\otimes$	W_3	=	$\Gamma_1 \oplus X_1 \oplus 2\Sigma_1$

members of the vector $\underline{k}$, then this set of EPMEs is transformed to a new set at each of the other members of the star of $\underline{k}'$.

In the computer program, the EPME is calculated for the identity star member of $\underline{k}'$ and all the unique star members of $\underline{k}$. The EPME is in general a 3x3 matrix (three components: x, y, z; and three polarizations or alternatively basis partners) and may be operated on by the appropriate rotation matrices of Table A2-3. To write down the explicit transformation, a group operation of the mth star member of the vector $\underline{k}$ is denoted by $\underline{R}_{\underline{k}_{m*}}$ and the identity star member of $\underline{k}'$ and ith star member of $\underline{k}$ of the EPME is denoted by $M_{1i}(\underline{k}'_{1*}, \underline{k}_{i*})$. The transformation of this EPME to the EPME of the jth star of $\underline{k}'$ and lth star of $\underline{k}$ is accomplished by

$$M_{jl}(\underline{k}'_{j*}, \underline{k}_{l*}) = \underline{R}_{\underline{k}'_{j*}} M_{1i}(\underline{k}'_{1*}, \underline{k}_{i*}) \underline{R}^{-1}_{\underline{k}'_{j*}} \tag{A2-7}$$

with $\underline{R}^{-1}$ the inverse operation to $\underline{R}$ and the lth star member of $\underline{k}$ determined by

$$\underline{R}_{\underline{k}'_{j*}} \underline{R}_{\underline{k}_{i*}} = \underline{R}_{\underline{k}_{l*}} \tag{A2-8}$$

The necessary group operations of the star members of the various reduced wave vectors are given in Table A2-6. This table is based on the irreducible wedge given in Figure A2-1, i.e. all the identity star members of the reduced wave vectors are contained in this wedge.

Table A2-6

Star Group Operations Generated from the Six Non-Equivalent BZ Points

BZ Point	Star Generation	Group Operations
Γ	R(0 0 0) = (0 0 0)	R = All 48 Operations
Δ	R(0 1 0) = (0 1 0)	R = 1 4 9 10 26 27 36 39
	= (0 0 1)	R = 7 13 17 21 32 40 43 47
	= (1 0 0)	R = 6 11 18 24 29 38 44 46
	= (0 -1 0)	R = 2 3 12 15 25 28 33 34
	= (0 0 -1)	R = 8 16 19 23 31 37 41 45
	= (-1 0 0)	R = 5 14 20 22 30 35 42 48
X	R(0 2 0) = (0 2 0)	R = 1 2 3 4 9 10 12 15 25 26 27 28 33 34 36 39
	= (0 0 2)	R = 7 8 13 16 17 19 21 24 31 32 37 40 41 43 45 47
	= (2 0 0)	R = 5 6 11 14 18 20 22 24 29 30 35 38 42 44 46 48
Σ	R(1 1 0) = (1 1 0)	R = 1 11 26 38
	= (1 -1 0)	R = 3 6 28 29
	= (-1 1 0)	R = 4 5 27 30
	= (-1 -1 0)	R = 2 14 25 35
	= (0 1 1)	R = 10 17 39 43
	= (0 -1 1)	R = 12 21 33 47
	= (0 1 -1)	R = 9 23 36 45
	= (0 -1 -1)	R = 15 19 34 41
	= (1 0 1)	R = 7 18 40 46
	= (1 0 -1)	R = 8 24 37 44
	= (-1 0 1)	R = 13 20 32 48
	= (-1 0 -1)	R = 16 22 31 42

Table A2-6 continued

BZ Point	Star Generation	Group Operations
L	R(1 1 1) = (1 1 1)	R = 1 14 15 16 17 18 25 38 39 40 41 42
	= (-1 1 1)	R = 3 5 10 13 19 24 27 29 34 37 43 48
	= (1 -1 1)	R = 4 6 7 12 22 23 28 30 31 36 46 47
	= (-1 -1 1)	R = 2 8 9 11 20 21 26 32 33 35 44 45
W	R(1 2 0) = (1 2 0)	R = 1 3 13 16 26 28 31 32
	= (2 1 0)	R = 5 11 19 21 30 38 41 47
	= (0 1 2)	R = 6 14 17 23 29 35 43 45
	= (0 2 1)	R = 10 12 22 24 33 39 42 44
	= (1 0 2)	R = 2 4 7 8 25 27 37 40
	= (2 0 1)	R = 9 15 18 20 34 36 46 48

APPENDIX III

EXPLICIT DERIVATION AND FORMULAE FOR THE EPME

We have shown in Chapter II, section 2-5, that the EPME expression to be evaluated numerically from (2-63) using SAPW basis functions is

$$M(\overset{\alpha'}{n}', \underline{k}'; \overset{\alpha}{n}, \underline{k}) = (4\pi)^2 \sum_{\underline{K}'} \sum_{\underline{K}} \sum_{\underline{R}'\in G_{\underline{k}'}} \sum_{\underline{R}\in G_{\underline{k}}} \sum_{s'} \sum_{s} C^{*\alpha'}_{n',s}(\underline{K}')\, C^{\alpha}_{n,s}(\underline{K})\, \Gamma^{\alpha'}_{n',s}(\underline{R}')\, \Gamma^{*\alpha}_{n,s}(\underline{R})$$

$$\sum_{\ell'} \sum_{\ell} \sum_{m'} \sum_{m} Y^{*}_{\ell' m'}(\theta_{\underline{R}'\underline{k}'}, \phi_{\underline{R}'\underline{k}'})\, Y_{\ell m}(\theta_{\underline{Rk}}, \phi_{\underline{Rk}}) \int_{\Omega} Y^{*}_{\ell' m'}\, \underline{\varepsilon}_{q\lambda} \cdot \hat{e}_r\, Y_{\ell m}\, d\Omega$$

$$i^{\ell'} i^{\ell} \quad \frac{j_{\ell'}(k'R_s)\, j_{\ell}(kR_s)}{u^{*}_{\ell'}(E'R_s)\, u_{\ell}(ER_s)} \int_0^{R_s} u^{*}_{\ell}(E', r) \frac{dV}{dr}\, u_{\ell}(E, r)\, r^2\, dr \qquad \text{(A3-1)}$$

By considering an arbitrary polarization vector of the form

$$\underline{\varepsilon}_{q\lambda} = a\hat{e}_x + b\hat{e}_y + c\hat{e}_z \qquad \text{(A3-2)}$$

we can consider the x, y, and z components of (A3-1) separately. This is done by remembering that

$$\hat{e}_r = \cos\phi\sin\theta\hat{e}_x + \sin\phi\sin\theta\hat{e}_y + \cos\theta\hat{e}_z \qquad \text{(A3-3)}$$

where the angular convention of the spherical harmonics is used. Taking the dot product between $\hat{e}_r$ and $\underline{\varepsilon}_{q\lambda}$ gives three separate angular parts, one for each component

$$Y^{*}_{\ell' m'}(\theta_{\underline{R}'\underline{k}'}, \phi_{\underline{R}'\underline{k}'})\, Y_{\ell m}(\theta_{\underline{Rk}}, \phi_{\underline{Rk}}) \int_{\Omega} Y^{*}_{\ell' m'}(\theta, \phi) \cos\phi\sin\theta\, Y_{\ell m}(\theta, \phi)\, d\Omega \qquad \text{(A3-4a)}$$

$$Y^{*}_{\ell' m'}(\theta_{\underline{R}'\underline{k}'},\phi_{\underline{R}'\underline{k}'})Y_{\ell m}(\theta_{\underline{Rk}},\phi_{\underline{Rk}})\int_{\Omega} Y^{*}_{\ell' m'}(\theta,\phi)\sin\phi\sin\theta Y_{\ell m}(\theta,\phi)d\Omega \quad \text{(A3-4b)}$$

$$Y^{*}_{\ell' m'}(\theta_{\underline{R}'\underline{k}'},\phi_{\underline{R}'\underline{k}'})Y_{\ell m}(\theta_{\underline{Rk}},\phi_{\underline{Rk}})\int_{\Omega} Y^{*}_{\ell' m'}(\theta,\phi)\cos\theta Y_{\ell m}(\theta,\phi)d\Omega \quad \text{(A3-4c)}$$

We shall derive explicitly the z-component expression to demonstrate how the final expressions were calculated. The following identities for the spherical harmonics and Legendre polynomials are based on unpublished notes of Trickey[50] for use in a $\underline{k}.\underline{p}$ energy band method. The spherical harmonics are of the Condon and Shortley convention[27] and are defined by

$$Y_{\ell m}(\theta,\phi) = C_{\ell m}P_{\ell m}(\cos\theta)\exp(im\phi) \quad \text{(A3-5a)}$$

where

$$C_{\ell m} = (-1)^{m}\left[\frac{(2\ell+1)}{4\pi}\frac{(\ell-m)!}{(\ell+m)!}\right]^{1/2} \quad \text{(A3-5b)}$$

and $P_{\ell m}$ are the associated Legendre polynomials.

The identities that are used in the angular integrals to invoke the orthogonality of the spherical harmonics are

$$\cos\theta Y_{\ell m} = \frac{C_{\ell m}}{(2\ell+1)}\left[\frac{(\ell-m+1)}{C_{\ell+1m}}Y_{\ell+1m} + \frac{(\ell+m)}{C_{\ell-1m}}Y_{\ell-1m}\right] \quad \text{(A3-6)}$$

$$\sin\theta Y_{\ell m} = \exp(i\phi)\frac{C_{\ell m}}{(2\ell+1)}\left[\frac{(\ell+m)(\ell+m-1)}{C_{\ell-1m-1}}Y_{\ell-1m-1} - \frac{(\ell-m+1)(\ell-m+2)}{C_{\ell+1m-1}}Y_{\ell+1m-1}\right] \quad \text{(A3-7)}$$

$$\sin\theta Y_{\ell m} = \exp(-i\phi)\frac{C_{\ell m}}{(2\ell+1)}\left[\frac{1}{C_{\ell+1m+1}}Y_{\ell+1m+1} - \frac{1}{C_{\ell-1m+1}}Y_{\ell-1m+1}\right] \quad \text{(A3-8)}$$

$$\sin\phi = 1/2i\ (\exp[i\phi] - \exp[-i\phi]) \quad \text{(A3-9)}$$

$$\cos\phi = 1/2\ (\exp[i\phi] + \exp[-i\phi]) \quad \text{(A3-10)}$$

$$\int_{\Omega} Y^{*}_{\ell' m'}(\theta,\phi)Y_{\ell m}(\theta,\phi)d\Omega = \delta_{\ell\ell'}\delta_{mm'} \quad \text{(A3-11)}$$

$$P_{\ell}(\cos\gamma) = \frac{4\pi}{2\ell+1}\sum_{m=-\ell}^{\ell} Y^{*}_{\ell m}(\theta_2,\phi_2)Y_{\ell m}(\theta_1,\phi_1) \quad \text{(A3-12)}$$

where $\cos\gamma = u = \cos\theta_1\cos\theta_2 + \sin\theta_1\sin\theta_2\cos(\phi_1-\phi_2)$ and $P_{\ell}(u)$ are the

Legendre polynomials. The greatest simplification of the spherical harmonic expressions is due to the next identity which is generally not well known, but which is proven by Trickey[50] in his unpublished notes

$$\cos\theta_1 \frac{dP_{\ell+1}}{du} - \cos\theta_2 \frac{dP_\ell}{du} = 4\pi \sum_{m=-\ell}^{\ell} \left[\frac{(\ell+m+1)(\ell-m+1)}{(2\ell+1)(2\ell+3)}\right]^{1/2} Y^*_{\ell m}(\theta_2,\phi_2) Y_{\ell+1 m}(\theta_1,\phi_1) \qquad \text{(A3-13)}$$

The LHS of (A3-13) may be simplified by using the following recursive relations of the Legendre polynomials

$$\frac{dP_\ell}{du} = \frac{(\ell+1)}{1-u^2}\,[\,uP_\ell - P_{\ell+1}] \qquad \text{(A3-14a)}$$

$$\frac{dP_\ell}{du} = \frac{\ell}{1-u^2}\,[\,P_{\ell-1} - uP_\ell] \qquad \text{(A3-14b)}$$

Therefore (A3-13) reduces to

$$\cos\theta_1 \frac{dP_{\ell+1}}{du} - \cos\theta_2 \frac{dP_\ell}{du} = \frac{(\ell+1)}{1-u^2}[\,P_\ell(\cos\theta_1 - u\cos\theta_2) + P_{\ell+1}(\cos\theta_2 - u\cos\theta_1)] \qquad \text{(A3-15)}$$

It is seen that we have an apparent singularity at $u = \pm 1$ (which corresponds to parallel or anti-parallel directions). However, by taking the appropriate limit of (A3-15) as $u \to \pm 1$, we may show that

$$\lim_{u\to\pm 1} \cos\theta_1 \frac{dP_{\ell+1}}{du} - \cos\theta_2 \frac{dP_\ell}{du} = (\pm 1)^\ell (\ell+1) \cos\theta_1 \qquad \text{(A3-16)}$$

By using (A3-6) in (A3-4c) and invoking (A3-11), we obtain

$$\begin{aligned}
&\sum_{\ell,\ell'} \sum_{m,m'} Y^*_{\ell' m'}(\theta_{\underline{R}'\underline{k}'},\phi_{\underline{R}'\underline{k}'}) Y_{\ell m}(\theta_{\underline{Rk}},\phi_{\underline{Rk}}) \int_\Omega Y^*_{\ell' m'} \cos\theta\, Y_{\ell m}\, d\Omega = \\
&\sum_\ell \sum_{m=-\ell}^{\ell} \Big(\left[\frac{(\ell-m+1)(\ell+m+1)}{(2\ell+1)(2\ell+3)}\right]^{1/2} Y^*_{\ell+1 m}(\theta_{\underline{R}'\underline{k}'},\phi_{\underline{R}'\underline{k}'}) Y_{\ell m}(\theta_{\underline{Rk}},\phi_{\underline{Rk}}) \\
&\quad + \left[\frac{(\ell-m+1)(\ell+m+1)}{(2\ell+1)(2\ell+3)}\right]^{1/2} Y^*_{\ell m}(\theta_{\underline{R}'\underline{k}'},\phi_{\underline{R}'\underline{k}'}) Y_{\ell+1 m}(\theta_{\underline{Rk}},\phi_{\underline{Rk}}) \Big)
\end{aligned} \qquad \text{(A3-17)}$$

The RHS of (A3-17) may be further simplified through the use of

(A3-13) and (A3-15)

$$\sum_{\ell} \frac{(\ell+1)}{1-u^2} [(P_{\ell+1}(\cos\theta_{\underline{Rk}}-u\cos\theta_{\underline{R}'\underline{k}'}) + P_{\ell}(\cos\theta_{\underline{R}'\underline{k}'}-u\cos\theta_{\underline{Rk}}))$$

$$- (P_{\ell+1}(\cos\theta_{\underline{R}'\underline{k}'}-u\cos\theta_{\underline{Rk}}) + P_{\ell}(\cos\theta_{\underline{Rk}}-u\cos\theta_{\underline{R}'\underline{k}'}))] \qquad (A3\text{-}18)$$

The reason that the terms are not combined in (A3-18) is that there are ℓ-dependent radial parts multiplying each term in the parentheses within the square brackets. Combining (A3-18) and (A3-1) gives for the final expression of the z component

$$M_z(\overset{\alpha'}{n}',\underline{k}';\overset{\alpha}{n},\underline{k}) = 4\pi i \sum_{\underline{K}'} \sum_{\underline{K}} \sum_{\underline{R}'\epsilon G_{\underline{k}'}} \sum_{\underline{R}\epsilon G_{\underline{k}}} \sum_{s'} \sum_{s} C^{*\alpha'}_{n',s}(\underline{K}')C^{\alpha}_{n,s}(\underline{K})\Gamma^{\alpha'}_{n',s}(\underline{R}')\Gamma^{*\alpha}_{n,s}(\underline{R})$$

$$\sum_{\ell} \frac{(\ell+1)}{1-u^2} [(P_{\ell+1}(\cos\theta_{\underline{Rk}}-u\cos\theta_{\underline{R}'\underline{k}'}) + P_{\ell}(\cos\theta_{\underline{R}'\underline{k}'}-u\cos\theta_{\underline{Rk}}))$$

$$\frac{j_{\ell+1}(k'R_s)j_{\ell}(kR_s)}{u^*_{\ell+1}(E'R_s)u_{\ell}(ER_s)}\int_0^{R_s} u^*_{\ell+1}(E',r)\frac{dV}{dr}u_{\ell}(E,r)r^2dr$$

$$- (P_{\ell+1}(\cos\theta_{\underline{R}'\underline{k}'}-u\cos\theta_{\underline{Rk}}) + P_{\ell}(\cos\theta_{\underline{Rk}}-u\cos\theta_{\underline{R}'\underline{k}'}))$$

$$\frac{j_{\ell}(k'R_s)j_{\ell+1}(kR_s)}{u^*_{\ell}(E'R_s)u_{\ell+1}(ER_s)}\int_0^{R_s} u^*_{\ell}(E',r)\frac{dV}{dr}u_{\ell+1}(E,r)r^2dr \quad] \qquad (A3\text{-}19)$$

For the M_x and M_y components of the EPME, we have applied the above methods and have obtained the following expressions

$$M_x(\overset{\alpha'}{n}',\underline{k}':\overset{\alpha}{n},\underline{k}) = 4\pi i \sum_{\underline{K}'} \sum_{\underline{K}} \sum_{\underline{R}'\epsilon G_{\underline{k}'}} \sum_{\underline{R}\epsilon G_{\underline{k}}} \sum_{s'} \sum_{s} C^{*\alpha'}_{n',s}(\underline{K}')C^{\alpha}_{n,s}(\underline{K})\Gamma^{\alpha'}_{n',s}(\underline{R}')\Gamma^{*\alpha}_{n,s}(\underline{R})$$

$$\sum_{\ell} \frac{(\ell+1)}{1-u^2} [(P_{\ell+1}(\cos\phi_{\underline{Rk}}\sin\theta_{\underline{Rk}}-u\cos\phi_{\underline{R}'\underline{k}'}\sin\theta_{\underline{R}'\underline{k}'}) +$$

$$P_{\ell}(\cos\phi_{\underline{R}'\underline{k}'}\sin\theta_{\underline{R}'\underline{k}'}-u\cos\phi_{\underline{Rk}}\sin\theta_{\underline{Rk}}))\frac{j_{\ell+1}(k'R_s)j_{\ell}(kR_s)}{u^*_{\ell+1}(E'R_s)u_{\ell}(ER_s)}\int_0^{R_s} u^*_{\ell+1}(E')\frac{dV}{dr}u_{\ell}(E)r^2dr$$

$$- (P_{\ell+1}(\cos\phi_{\underline{R}'\underline{k}'}\sin\theta_{\underline{R}'\underline{k}'}-u\cos\phi_{\underline{Rk}}\sin\theta_{\underline{Rk}}) +$$

$$P_{\ell}(\cos\phi_{\underline{Rk}}\sin\theta_{\underline{Rk}}-u\cos\phi_{\underline{R}'\underline{k}'}\sin\theta_{\underline{R}'\underline{k}'}))\frac{j_{\ell}(k'R_s)j_{\ell+1}(kR_s)}{u^*_{\ell}(E'R_s)u_{\ell+1}(ER_s)}\int_0^{R_s}u^*_{\ell}(E')\frac{dV}{dr}u_{\ell+1}(E)r^2dr\ ] \tag{A3-20}$$

and

$$M_y(\overset{\alpha'}{n'},\underline{k}';\overset{\alpha}{n},\underline{k}) = 4\pi i\sum_{\underline{K}'}\sum_{\underline{K}}\sum_{\underline{R}'\varepsilon G_{\underline{k}'}}\sum_{\underline{R}\varepsilon G_{\underline{k}}}\sum_{s'}\sum_{s}C^{*\alpha'}_{n',s}(\underline{K}')C^{\alpha}_{n,s}(\underline{K})\Gamma^{\alpha'}_{n',s}(\underline{R}')\Gamma^{*\alpha}_{n,s}(\underline{R})$$

$$\sum_{\ell}\frac{(\ell+1)}{1-u^2}\ [\ (P_{\ell+1}(\sin\phi_{\underline{Rk}}\sin\theta_{\underline{Rk}}-u\sin\phi_{\underline{R}'\underline{k}'}\sin\theta_{\underline{R}'\underline{k}'}) +$$

$$P_{\ell}(\sin\phi_{\underline{R}'\underline{k}'}\sin\theta_{\underline{R}'\underline{k}'}-u\sin\phi_{\underline{Rk}}\sin\theta_{\underline{Rk}}))\frac{j_{\ell+1}(k'R_s)j_{\ell}(kR_s)}{u^*_{\ell+1}(E'R_s)u_{\ell}(ER_s)}\int_0^{R_s}u^*_{\ell+1}(E')\frac{dV}{dr}u_{\ell}(E)r^2dr$$

$$-\ (P_{\ell+1}(\sin\phi_{\underline{R}'\underline{k}'}\sin\theta_{\underline{R}'\underline{k}'}-u\sin\phi_{\underline{Rk}}\sin\theta_{\underline{Rk}}) +$$

$$P_{\ell}(\sin\phi_{\underline{Rk}}\sin\theta_{\underline{Rk}}-u\sin\phi_{\underline{R}'\underline{k}'}\sin\theta_{\underline{R}'\underline{k}'}))\frac{j_{\ell}(k'R_s)j_{\ell+1}(kR_s)}{u^*_{\ell}(E'R_s)u_{\ell+1}(ER_s)}\int_0^{R_s}u^*_{\ell}(E')\frac{dV}{dr}u_{\ell+1}(E)r^2dr\ ] \tag{A3-21}$$

Equations (A3-19), (A3-20), and (A3-21) have been coded into the EPME program (see Appendix IV) together with the appropriate limiting expression (A3-16).

APPENDIX IV

DESCRIPTION OF COMPUTER PROGRAMS AND CODES

All numerical calculations have been done using a set of three programs. Two of the programs have been used and tested in many different calculations. The other program was written by the author during the course of this calculation.

One of the established programs calculates the energy bands and electronic wave functions based on the APW model, using computer codes developed by Wood and others,[51,3] and made self-consistent and modified by Connolly and others.[52,23,24] In the course of this work, it was found necessary to modify the numerical precision (from single to double) of the card output of the potential, eigenvalues, and basis function coefficients. Also the basis function coefficients had to be normalized properly for use outside of the APW program [using (2-25)].

The other established program is Koehler's SCH code[14] based on the formalism outlined in Appendix II. This program calculates a set of phonons on any given reciprocal space mesh and at any temperature, given the crystal structure, lattice parameter, Lennard-Jones parameters, and the temperature. This code has been used and modified by Trickey[50] for development of certain point transform problems.

The third program was written entirely by the author except for certain subroutines which were borrowed from the APW program to perform similiar tasks. This program calculates the EPME over the entire Brillouin zone. Presently all s-like band to p-like band transitions or all p-like band to s-like band transitions can be done, given that one of the bands is full. The calculation of the perturbed phonon spectrum is also done within this program.

It should also be mentioned that the APW and EPME programs use symmetrized basis functions. Group theory and projection operators are used to specify lists of contributing reciprocal lattice vectors at any given reduced zone vector. This "specification deck" is used as input to the APW and the EPME programs.

All programs are written in FORTRAN and have been compiled with I.B.M.'s FORTRAN H-Extended compiler and linkedited and overlayed with I.B.M.'s F-128 linkage editor. Numerical precision is double precision throughout all programs (approximately 16 decimal digits).

The EPME program has been overlayed and arranged to run in 128K bytes of core. The program is also designed to be restartable at any point in the actual EPME calculation. The typical running time for the calculations done in this dissertation was 70 minutes CPU (360/M195) which is approximately 140 minutes CPU (370/M165) for all the p to s transitions on a 32 point reciprocal space mesh. The APW calculations ran about 5 to 10 minutes CPU (370/M165) depending on the desired convergence. The amount of required core depended on the basis size. The SCH calculations ran typically less than a minute and in about 150K of core.

Numerical integration and differentiation are done in the EPME program. The potential has to be differentiated, which is done by using an eleven point Lagrangian differentiation algorithm.[53] The routine was checked against a known function ($f(r) = 1/r \exp[-ar]$) whose exact derivative is calculable. The numerical and exact derivative values agreed to full double precision for all values of r tested. This function was chosen as a test case because it closely resembles the numerical form of the self-consistent APW potential. The numerical integration routine is the same as that used in the APW program and is based on a five point Newton-Cotes integration algorithm.[54] The radial wave function of the Schrödinger eqn. is solved by the Numerov method[3] in a subroutine also borrowed from the APW program.

All program labeling and numbering conventions of the energy bands and electron wave vectors follow BSW[29] (see Appendix II) and are based on the "specs" deck used for both the APW and EPME calculation. The same notation is used in labeling the dispersion curves and phonon wave vectors.

LIST OF REFERENCES

1. Golibersuch, D.C., Phys. Rev. 157, 532 (1967).

2. Slater, J.C., Phys. Rev. 51, 846 (1937).

3. Mattheiss, L.F., Wood, J.H., and Switendick, A.C. in Methods in Computational Physics, edited by B. Adler, S. Fernbach, and M. Rotenberg (Academic Press, New York 1963), Vol. 8, p.63.

4. Fröhlich, H., Phys. Rev. 79, 845 (1950).

5. Sinha, S.K., Phys. Rev. 169, 477 (1968).

6. Toya, T., J. Res. Inst. Catalysis, Hokkaido University, 6, 161 (1958).

7. Pick, R.M., Cohen, M.H., and Martin, R.M., Phys. Rev. B 1, 910 (1970).

8. see the excellent review article and reference list of Chapter 7 in Dynamics of Perfect Crystals, by G. Venkataraman, L.A. Feldkamp, and V.C. Sahni (MIT Press, Boston 1975).

9. Born, M. and Oppenheimer, J.R., Ann. Physik 84, 457 (1927).

10. Koehler, T.R. and Nesbet, R.K., Phys. Rev. 135, A638 (1964).

11. Slater, J.C., Phys. Rev. 81, 385 (1951).

12. Connolly, J.W.D., in Modern Theoretical Chemistry, edited by G. Segal (Plenum Press, New York 1976), Vol. 7, p.105.

13. Nordheim, L., Ann. Phys. 9, 607 (1931).

14. Koehler, T.R., Phys. Rev. Lett. 17, 89 (1966).

15. Lennard-Jones, J.E. and Ingham, A.E., Proc. Roy. Soc.(London) A107, 612 (1925).

16. Ziman, J.M., Electrons and Phonons, (Oxford Press, London 1960).

17. Johnson, F.A., Proc. Roy. Soc.(London), A310, 79 (1969).

18. Chester, G.V., Advan. Phys. 10, 357 (1961).

19. Sham, L.J. and Ziman, J.M., Solid State Phys. 15, 221 (1963).

20. Englman, R., Phys. Rev. **129**, 551 (1963).

21. Kittel, C., *Introduction to Solid State Physics*, (Wiley, New York 1971).

22. see for example D. Pines, *Elementary Excitations in Solids*, (Benjamin, New York 1964).

23. Trickey, S.B., Green, F.R.,Jr, and Averill, F.W., Phys. Rev. B **8**, 4822 (1973).

24. Sabin, J.R., Worth, J.P., and Trickey, S.B., Phys. Rev. B **11**, 3658 (1975).

25. Gaspar, R., Acta Phys. Hung. **3**, 263 (1954); Kohn, W. and Sham, L.J., Phys. Rev. **140**, A1133 (1965).

26. Schwarz, K., Phys. Rev. B **5**, 2466 (1972).

27. Condon, E.U. and Shortley, G.H., *The Theory of Atomic Spectra* (Cambridge Press, Cambridge 1951).

28. Fröhlich, H., Proc. Phys. Soc. (London) **64**, 129 (1952); Proc. Roy. Soc. A **215**, 291 (1952).

29. Bouckaert, L.P., Smoluchowski, R., and Wigner, E.P., Phys. Rev. **50**, 58 (1936).

30. Hedin, L. and Lundqvist, S., Solid State Phys. **23**, 1 (1969).

31. Taylor, P.L., *A Quantum Approach to the Solid State* (Wiley, New York 1974).

32. Migdal, A.B., Soviet Phys. JETP (English Transl.) **7**, 996 (1958).

33. Scott, T.A., private communication, 1975.

34. Kenney, J., "The Energy Band Problem for a Deformed Lattice", in Mass. Inst. Tech. SSMTG Semi-Ann. Progr. Rep. **62**, 26 (1966).

35. Slater, J.C., *Symmetry and Energy Bands in Crystals* (Dover, New York 1972) p.225.

36. Pollack, G.L., Rev. Mod. Phys. **36**, 748 (1964).

37. Endoh, Y., Shirane, G., and Skalyo, J. Jr., Phys. Rev. B **11**, 1681 (1975).

38. Fujii, Y., Lurie, N.A., Pynn, R., and Shirane, G., Phys. Rev. B **10**, 3647 (1974).

39. Barker, J.A. and Henderson, D., Rev. Mod. Phys. **48**, 587 (1976).

40. Worth, J.P., Merry, C.L., Trickey, S.B., and Sabin, J.R., to be published.

41. Sambe, H. and Felton, R.H., J. Chem. Phys. 62, 1122 (1975).

42. Koehler, T.R., Phys. Rev. 165, 942 (1968).

43. Koehler, T.R., in "Proceeding of the International School of Physics Enrico Fermi, Course 55", edited by S. Califano (Academic Press, New York 1975).

44. de Boer, J., Physica 14, 139 (1948).

45. Hirschfelder, J., Curtis, C.F., and Bird, R.B., Molecular Theory of Gases and Liquids (Wiley, New York 1964).

46. Kihara, T. and Koba, S., J. Phys. Soc. Japan 7, 348 (1952).

47. Zak, J., Phys. Rev. 151, 464 (1966).

48. von der Lage, F.C. and Bethe, H.A., Phys. Rev. 71, 612 (1947).

49. Lax, M., Symmetry Principles in Solid State and Molecular Physics (Wiley, New York 1974).

50. Trickey, S.B., private communication, 1975.

51. Wood, J.H., Ph.D. Dissertation, Massachusetts Institute of Technology (1958).

52. Connolly, J.W.D., Ph.D. Dissertation, University of Florida (1968).

53. Bickley, W.G., Math. Gaz. 25, 19 (1941).

54. Hamming, G., Numerical Methods for Scientists and Engineers (McGraw-Hill, New York 1962), p.127.

BIOGRAPHICAL SKETCH

Joseph Patrick Worth was born on 25 July 1949 in Salzburg, Austria. He attended various public and army base schools in Europe and the United States. He was graduated from Cuyahoga Falls High School in Cuyahoga Falls, Ohio on 9 June 1967. From October 1967 to June 1969, he served in the United States Army and was then honorably discharged. He enrolled at the University of Akron in September 1969 and was graduated in June 1972 with a Bachelor of Science (Physics) and in June 1973 with a Master of Science.

In September 1973, he began Ph.D. graduate study at the University of Florida. He joined the Quantum Theory Project in June 1974 and has been working toward his degree since that time.

I certify that I have read this study and that in my opinion it conforms to acceptable standards of scholarly presentation and is fully adequate, in scope and quality, as a dissertation for the degree of Doctor of Philosophy.

Sam B. Trickey

S.B. Trickey, Chairman
Associate Professor of Physics

I certify that I have read this study and that in my opinion it conforms to acceptable standards of scholarly presentation and is fully adequate, in scope and quality, as a dissertation for the degree of Doctor of Philosophy.

N.Y. Öhrn
Professor of Chemistry and Physics

I certify that I have read this study and that in my opinion it conforms to acceptable standards of scholarly presentation and is fully adequate, in scope and quality, as a dissertation for the degree of Doctor of Philosophy.

J.R. Sabin
Associate Professor of Physics
and Chemistry

I certify that I have read this study and that in my opinion it conforms to acceptable standards of scholarly presentation and is fully adequate, in scope and quality, as a dissertation for the degree of Doctor of Philosophy.

TA Scott

T.A. Scott
Professor of Physics

I certify that I have read this study and that in my opinion it conforms to acceptable standards of scholarly presentation and is fully adequate, in scope and quality, as a dissertation for the degree of Doctor of Philosophy.

C. E. Reid

C.E. Reid
Associate Professor of Chemistry

This dissertation was submitted to the Graduate Faculty of the Department of Physics in the College of Arts and Sciences and to the Graduate Council, and was accepted as partial fulfillment of the requirements for the degree of Doctor of Philosophy.

December, 1976

Dean, Graduate School

UNIVERSITY OF FLORIDA
3 1262 08666 924 8